

Response to Review #1

We thank Dr. Kochendorfer for his constructive and insightful comments. Our response to each of the comments is stated. The response is given within the %%%--- ---%%% symbols below. In addition to the points raised by both reviewers, we found small errors in the calculation of the spectral ratio in Table 2 for all corrections and sharpened criteria for the CSAT3 at Risø, which have now been corrected.

Regards,
The authors

General Comments

“A method to assess the accuracy of sonic anemometer measurements” evaluates turbulence power spectra to estimate biases in sonic anemometer measurements. As energy is transformed from large eddies to the smallest eddies where it is finally dissipated, within a range of ‘middle’ sized eddies there energy flows from larger scales of turbulence to smaller scales. This middle range of turbulence is called the inertial subrange, and within it the flow of energy is relatively constant with turbulence scale. Because of this, turbulence within the inertial subrange follows predictable laws. In the manuscript these laws are used to evaluate turbulence measurements recorded using different types of sonic anemometers at different sites. This is done in part because a standard for the measure of turbulence is not readily and commonly available.

The manuscript is well written, with appropriate and clear figures, and is generally well composed. The topic is certainly worth investigating, as sonic anemometers are relied upon for measuring eddy covariance fluxes and turbulence, and many studies have cast the accuracy of their measurements into question. The technique proposed is somewhat novel, at least as a method of evaluating sonic anemometer measurements, and as such it may be useful. The technique suffers, by the authors’ own admission, of being a relative measure, rather than an absolute one; the ideal ratio of 4/3 between the W and U spectra can be achieved when both W and U are incorrect, just as long as they are incorrect to the same degree. In addition, the method can only be applied to measurements that are recorded well above the surface, in well-developed turbulence, where the inertial subrange is clearly distinguishable. However the manuscript confronts these shortcomings directly, and demonstrates how the technique is still quite useful for evaluating the accuracy of sonic anemometer measurements.

%%%--- We acknowledge the reviewer for his general comments, all being positive. We also agree with the reviewer in that this is a very important topic as sonic anemometer measurements are the backbone of turbulence studies. As the reviewer points out, our method does suffer of being a relative measure, as we clearly stated it, but does help identifying non-accurate measurements of velocity fluctuations --- %%%

Specific Comments

P. 2, l. 34 – 35. Although an ATI was briefly evaluated in Kochendorfer et al. (2012), Kochendorfer et al. (2012) derived their corrections using three identical R. M. Young anemometers, by changing the orientation of the center anemometer and assuming that the outer two anemometers were capable of accurately measuring the horizontal wind speed when the angle of attack was near-zero. This is the method referred to as “the third variant” used by Nakai and Shimoyama (2012) in the manuscript (l. 22 – 31), and was originally presented by Meyers and Heuer, (2006). Regarding the “busy” setup, turbulent statistics can be compared when all anemometers are oriented vertically to evaluate biases in the wind

field (e.g. Kochendorfer et al., 2013).

%%%--- Indeed, we also called it “a third variant”. The sentence about the Kochendorfer et al. (2012) study was moved to the same paragraph as the Nakai and Shimoyana (2012) study, to clarify that the main focus of this study was to intercompare anemometers of the same brand. We added the Meyers and Heuer (2006) study to the reference list, but note that the study is a short abstract to a conference and we rely on the editor to judge whether this is acceptable as a reference in AMT. We also added the citation to Kaimal et al. (1990), who also used sonic anemometers of the same brand mounted at a close distance to each other, to evaluate potential systematic errors. Concerning “the” busy setup, we would like to maintain a weakened version of this statement, although we agree with Dr. Kochendorfer that the observations can be compared. We merely point out that the extra booms and clamps needed for multiple sonic observations at close distance may introduce significant small-scale gradients. When looking for very small errors, it is hard to judge a priori whether such gradients can bias the result, and we see this issue as one of the very few potential problems to the investigations presented by both Kochendorfer et al. (2012) and Nakai and Shimoyama (2012). Since we have no quantitative analysis to back up this statement, we have rewritten the sentence to: “Also, it is hard to evaluate whether the somewhat “busy” setup with several sonic anemometers in a small area could lead to additional and larger flow distortions than those using a single sonic anemometer.” ---%%%

P. 3, l. 2. Frank et al. (2013) was unique in that the anemometers were re-oriented to check for self-consistency between different measurement axes – their experiment was not similar to the Kochendorfer et al. (2012) experiment, which only used data with zero angle of attack.

%%%--- We did not state that the experiment was similar, but that the *setup* was similar. In the new version of the manuscript, the citation to the Kochendorfer et al. (2012) study is moved to the paragraph where we introduce the Nakai and Shimoyama (2012) study ---%%%

P. 3, l. 4. Explain what is mean by “a combination of all three methods”.

%%%--- We categorize previous work in characterizing sonic anemometer errors in three broad categories: (i) wind-tunnel calibration, (ii) comparison of different brands of sonic anemometers to each other and (iii) tilting sonic anemometers of the same brand relative to each other. “A combination of all three methods” simply means that all these methods were used in Horst et al. (2015). Since this statement is now closer to the top of the paragraph, where the three methods are stated, we hope that our wording can now be understood ---%%%

P. 3, l. 13. This is a semantic, but still significant issue: The manuscript presents a new method for evaluating biases in sonic anemometers, but it is misleading to call it a ‘new reference’. For example, if two sonic anemometers differ in their measurements, this method may not necessarily be capable of determining which one is more accurate, as it does not include an independent measurement of the wind speed; it is possible that both anemometers could have a 4/3 slope, and yet still differ from each other. The manuscript would be stronger and more accurate if descriptions of the new method as a ‘reference’ (e.g. p. 3, l. 14 and l. 16) are reworded.

%%%--- We agree with the reviewer and have changed all “reference” entries to “method” in the revised manuscript ---%%%

P. 3, l. 31. I’m confused by this: “all one-point correlations between velocity components become zero”. This would imply that the momentum flux ($u'w'$) is zero within the inertial subrange, but that doesn't

sound possible. Please explain. Perhaps “become zero” should be reworded as “tend toward zero”?

%%-% We agree with the reviewer that this was unclearly formulated. In the revised version it is now stated “Turbulence is locally isotropic within this range, which means that all beyond that wavenumber all one-point cross-spectra between different velocity components approach zero. For example, the cross-spectrum between u and w decreases like $k_1^{-7/3}$, which is more rapid than F_u and the bulk of the momentum flux uw is located at a wavenumber lower than the inertial subrange” ---%%-%

P. 6, l. 22 and elsewhere. Change “Measurements are collected” to “Measurements were collected”. Events that occurred in the past should be described using the past tense. See <https://www.nature.com/scitable/topicpage/effective-writing-13815989> for examples and further explanation. All of the description of the work that was performed should be written in the past tense – this includes the majority of Sections 3, 4, and 5.

%%-% Changed as suggested by the reviewer ---%%-%

P. 7, l. 2. How were the effects of the wind turbines on the spectra evaluated or ruled out? It might be worth including something in the manuscript describing the evaluation of the spectra or distances and wind directions.

%%-% As recommended by the reviewer, in Sect. 3 we have added information regarding the wind direction sectors where possible wind turbine wakes can be found. For the CSAT3 at the Risø site, we have studied the potential effect of wakes on the observation in quite some detail and judged that the influence is negligible. First, the observation height is low compared to the hub height of the turbine and the distance to the closest turbine quite long. For the other sites, the wake sectors are harder to exclude. We now show in Figs. 4, 5, and 9 the wake sectors for the USA-1 at Risø and CSAT3 at Nørrekær Enge. The ratios computed in Table 2 now exclude all the possible wake-affected sectors for the USA-1 at Risø and for the CSAT3 at Nørrekær Enge ---%%-%

Figure 3. It is probably clearer to denote the right and left panels using letters (a and b), rather than right and left. The same can be said for the other paired figure panels.

%%-% Changed as suggested by the reviewer ---%%-%

P. 9, l. 12. Replace “wind conditions” with “wind direction”. And as Figure 4 shows, this statement isn’t strictly true. I get the general idea, but perhaps it should be written more precisely.

%%-% We have reformulated the sentence as recommended by the reviewer. However we did mean wind conditions because the turbulence conditions change noticeable with wind direction at this site. We have moved the sentence following that pointed out by the reviewer so that the reader understands what we mean by wind conditions ---%%-%

P. 12, l. 14. “we limit the range to a close to noise-free wavenumber” is grammatically incorrect – the sentence should probably end with, “a close to noise-free wavenumber range”, but then it becomes even more verbose. Rewrite the entire sentence improve clarity, brevity, and grammar. Here’s a suggestion:

“The wavenumber range was limited to exclude noise apparent at higher wavenumbers ($k_1 > 1 \text{ m}^{-1}$).”

%%-%--- Corrected as suggested by the reviewer ---%%%

P. 14, l. 17. Change, “only those spectra, which showed...” to, “only those spectra that showed...”.

%%-%--- Corrected as suggested by the reviewer ---%%%

P. 14, l. 20 (odd break in the line numbers here, perhaps due to a premature page break or the conversion to pdf). Change “spectra are calculated” to the past tense, “spectra were calculated”.

%%-%--- The odd line numbers are a result of the latex style of the journal. The tense was changed as suggested by the reviewer ---%%%

P. 15, l. 27 – 28. This is presumably only true when the measurements support the existence of a clearly defined inertial subrange. It seems like a bit of a chicken and egg problem– if the inertial subrange isn’t easily identified, is it because the measurements are compromised, or because the turbulence doesn’t follow the textbook?

%%-%--- We agree with the reviewer that this might seem like a chicken and egg problem. In our experience, it is easy to see a well-defined inertial subrange in the velocity spectra, when this does exist. We have therefore added “, provided that an inertial subrange is clearly apparent.” to the sentence ---%%%

P. 15, l. 39 (last line of p.15 – another weird brake in the line numbers here). No criticism here, just a note to the authors: Many of us interested in this type of work are hoping that LIDAR measurements will still provide a true wind velocity reference – please keep working on them! Tom Horst told me about this approach long ago, and I’m still waiting to see what comes of it...

%%-%--- Thanks for the comment. We plan to submit manuscripts where we show the benefits of laser anemometry for turbulence measurements and their potential to serve as a true reference ---%%%

References

Kochendorfer, J., Meyers, T. P., Frank, J. M., Massman, W. J., and Heuer, M. W.: Reply to the Comment by Mauder on “How Well Can We Measure the Vertical Wind Speed? Implications for Fluxes of Energy and Mass”, *Boundary- Layer Meteorology*, 147, 337-345, 2013.

Meyers, T. P. and Heuer, M.: A field methodology to evaluate sonic anemometer angle of attack errors, 27th Conference on Agric For Meteorol, San Diego, California, 2006.

Response to Review #2

We also thank anonymous reviewer #2 for the constructive comments and suggestions to the manuscript. Here our response to the comments. The response is given within the %%%--- ---%%% symbols. In addition to the points raised by both reviewers, we found small errors in the calculation of the spectral ratio in Table 2 for all corrections and sharpened criteria for the CSAT3 at Risø, which have now been corrected.

Regards,
The authors

General Comments

In this paper, the authors present a novel methodology to evaluate the relative accuracy of u , v , and w measurements from a sonic anemometer by applying Kolmogorov theory to the relative magnitude of the u , v , and w spectra within the inertial subrange. Based on that theory, the v and w spectra should be $4/3$ the magnitude of the u spectra. Using field data from Metek USA-1 and CSAT3 sonic anemometers at different towers, different field sites, without any shadowing correction, with shadowing correction, and with path averaging correction, the $4/3$ relationship was tested. For the Metek, while the uncorrected anemometer was much lower than $4/3$ for the w -to- u relationship, after applying a wind tunnel based calibration provided by the manufacturer this relationship becomes $\sim 4/3$. For the uncorrected CSAT3, the w -to- u relationship is a little close to $4/3$ than was the case for the uncorrected Metek, but after applying a shadowing correction, the ratio is still lower than $4/3$, being ~ 1.2 . Thus, the CSAT3 correction could be interpreted as providing only a partial amount of the correction required to achieve a $4/3$ relationship.

%%%--- Thanks for this comment. This is a good way to summarize the main findings of our analysis ---
%%%

This is a very novel idea, and has the potential to be fairly influential in the discipline. There are two items that seem very important that should be given more emphasis. First, this technique is among the few that does not require a comparison between one anemometer and another. Rather, it can be applied for any single anemometer at more-or-less any field site (I recognize that this is mentioned in the paper, but this is EXTREMELY important, so make sure there is no doubt the reader appreciates how powerful this statement is).

%%%--- We agree with the reviewer. We now include the following sentence in the abstract “and does not require the use of another measurement as reference” to further highlight the advantage of the method ---
%%%

Second, because this methodology is entirely based on Kolmogorov theory about the $4/3$ rasion between w - u and v - u spectra, it should be emphasized that in general all of the results from the v - u tests conform to this theory. While the reader must evaluate results such as Table 2 to determine whether w - u ratios of $\sim 1.0, \sim 1.1, \sim 1.2$ are evidence of underestimated w measurements, it is crucial to note that the v - u ratios are almost entirely $4/3$ for all cases. This gives a lot of credibility that the theory of isotropy is correct, and that the $4/3$ standard is reasonable.

%%%--- As suggested by the reviewer, we now state for each of the cases analyzed that the v to u spectra ratios are always close to $4/3$ irrespectively of the correction type or criteria used for filtering ---%%%

One improvement that will be necessary is to better clarify the differences between $4/3$, $5/3$, and $2/3$

slopes in the inertial subrange. I was completely confused upon my first reading, and I had to consult my Kaimal and Finnigan (1994) book to sort this out. While it is clear from Equation 1 that the slope of the inertial subrange is $-5/3$, figure 1 is a $-2/3$ slope, which presumably is because it is a “frequency weighted” spectra where the y-axis is actually spectra multiplied by wave number. This is related to second sentence in section 5.1, where the frequency-weighted spectra is multiplied by $k^{(2/3)}$ to give a straight line. This is entirely confusing unless the reader recognizes that it is already multiplied by $k^{(3/3)}$, which is essentially $k^{(5/3)}$, i.e., it makes the $-5/3$ slope in Equation 1 appear as a flat line. Yet, all of these details are rather unimportant when compared to the $4/3$ value in equation 2, which is actually written as $3/4$, but constitutes the most important relationship of the paper. This is the assumption from which all of the conclusions of this paper are drawn from. In summary, the reader should not have to consult Kaimal and Finnigan (1994) to sort out the meaning of the different ratios in this paper.

%%-- We understand the readers could be confused. We now include a statement in the caption of Fig. 1 so that the reader understands why the slope of this wavenumber pre-multiplied spectra is $-2/3$. When first presenting the computed spectra (for the USA-1 at Risø), we also add that these are flattened by multiplying by $k^{1/2}$ in contrast to the spectra in Fig. 1 --%%

I would recommend that more quantitative techniques be used to ensure that spectra included in the analyses conform to the theoretical $-5/3$ slope. One suggestion is that rather than only fitting a 0th order polynomial, a better method is to fit a 1st order polynomial with statistical software, then to test for the statistical significance of the 1st order coefficient. If, for example, the p-value for the 1st order (i.e., slope) coefficient is > 0.05 , it could be considered non-significant, and then it could essentially be concluded that the slope of the inertial subrange cannot be distinguished from $-5/3$. Once this is done, using arguments similar to model selection analysis, the 1st order polynomial model can then be reduced to the 0th order model currently described in the paper. In a manner, the goal of this is similar to the “sharpened” criteria in section 5.2/Table 2. The benefit of the statistical criteria is that it provides a defensible justification as to which 10-min periods should be included in the analysis based on their inertial subrange. Another similar idea could be to use a statistical break-point or change-point analysis for each 10-min period to determine the range over which the inertial subrange slope is $-5/3$ (i.e., use statistics to optimize the range of the inertial subrange for each 10-min period). This seems more complicated to me, but it could also work.

%%-- Although we understand that the selection of the wavenumber range did not appear quantitative, we have chosen not to follow this recommendation. As the reviewer points out, the goal of the recommendation is similar to our “sharpened” criterion, and we have chosen to focus on this selection. First, we now include the sharpened criteria to all sites in Table 2. Second, we now clarify at the beginning of section 5 (third paragraph) that the sharpened criteria are indeed used to filter out 10-min samples where the spectra do not follow the expected behavior within the inertial subrange. The strength of the sharpened criteria is that one might have slopes close to $-5/3$ outside the inertial subrange and so the uw-co-covariance test aids in determining the closeness of the selected range to conform to isotropy. As stated in the Discussion, several other selections have been tried with no difference in the result. See also our answer to the reviewer’s specific comment “Page 11 line 22” regarding the choice of the thresholds for the sharpened criteria: there we show the sensitivity of the results to the thresholds in the sharpened criteria. --%%

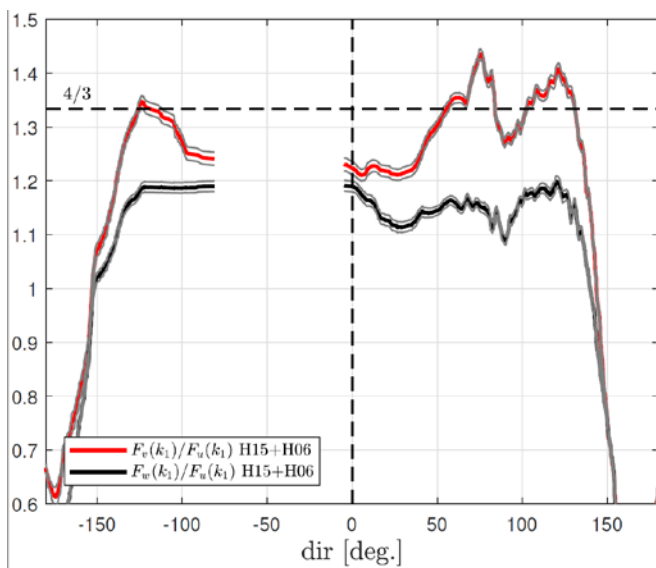
A more quantitative approach than a running mean such as in Figures 4, 5, 7, and 9 or mean/standard deviation such as in Table 2 would improve the interpretation that the results are statistical different/similar to $4/3$. One suggestion I have for the figures is to replace the running mean with a local (i.e., LOESS or LOWESS) regression.

This is a statistical technique that provides results similar to a running mean, but it also comes with confidence intervals. Thus, a similar figure could be produced, but with the added benefit that for any wind

direction it can be tested whether or not the best fit line is significantly different from $4/3$. A great example is figure 7 (right frame) where obviously for some wind directions neither the red or black lines are even close to $4/3$, but for other directions the red is similar to $4/3$. A LOESS fit would give a quantitative metric to determine where this is significantly different from $4/3$ and where it is significantly similar.

%%%--- We understand the suggestion of the reviewer. We have actually performed loess fits for the USA-1 at Risø and for the CSAT3 at Nørrekær Enge in the original manuscript (so it is now stated that these are the fits) and the estimation of the standard errors of such fits in Figs. 4, 7, and 9 and found that they were very small and difficult to discern when plotted besides the fit. For completeness, we now anyway provide some numbers related to such standard errors in the caption of the above mentioned figures ---%%%

%%%--- We agree with the suggestion of the reviewer. We have now implemented loess fits for all sites. In addition, we have now performed the estimation of the standard errors and confidence intervals of the fits for the values in Figs. 4, 7, and 9 and found that they were very small and difficult to discern when plotted besides the fit. For completeness, we now provide the standard errors in the caption of the above mentioned figures. When adding the 95% confidence interval, we have to assume that all the observations are independent, which is likely not the case. However, the observations are indeed significantly different from $4/3$ for most wind directions; please see the example below for the CSAT3 at the Risø site (the grey lines show the error range for the 0.95 confidence interval) ---%%%



I would encourage the authors to reconsider their interpretation of the Huq et al. (2017) paper. While it is correct that those results suggest a magnitude of correction similar to Horst et al. (2015) (i.e., 3-7% as mentioned in their abstract, or $\sim 6\%$, which is the average of second column of their Table 2), one important distinction is that when Huq et al. (2017) applied the Kaimal (1979) and Wyngaard and Zhang (1985) corrections to their numerically simulated data, the improvement in relative error was rather small (i.e., 2.4-3.4% correction, as derived from their Table 2). Frank et al. (2016) presented data from seven sites around North and Central America where these corrections increased the w measurements by 4.5-6.8% (their Table 2). While it takes a bit of interpretation to compare the results from these papers, one interpretation could be that the numerically simulated turbulence in Huq et al. (2017) tends to produce corrections (either Kaimal or Wyngaard) that are less than what are typically observed in nature. Thus, while an overall correction of $\sim 6\%$ is similar to that of Horst et al. (2015), the Kaimal/Wyngaard correction only accounts for $\sim 50\%$ of this. From this perspective, the findings of Huq et al. (2017) are very similar to

those of this paper, which is to say, the currently accepted CSAT3 corrections do improve w measurements, but perhaps only provide a portion of the correction that is ultimately required.

--- In the introduction, we would not like to go beyond the interpretation given by Huq et al. (2017) when they summarize their findings, and therefore, we have left the text as it was in the original submission. In the Discussion we have changed the formulations to be more precise (the new version is included in the bottom of this answer).

The abstract of Huq et al. (2017) states that “A comparison of the corrections for transducer shadowing proposed by both Kaimal et al. (*Proc Dyn Flow Conf*, 551–565, 1978) and Horst et al. (*Boundary-Layer Meteorol* 155:371–395, 2015) show that both methods compensate for **a larger part** of the observed error, but do not sufficiently account for the azimuth dependency.”

Further, the authors state in the last paragraph on page 23: “For the standard deviation of the w -component, Horst et al. (2015) report a relative error of between 3 and 5%, which is **almost the same** as our error. We suspect the error from our numerical experiment is slightly larger because the turbulence intensity is not quite as large as in the field, where more intense turbulence tends to weaken flow-distortion effects.”

We have written “Huq et al. (2017) presented a novel approach for estimating the accuracy of the CSAT3 by using numerical simulations. The results of the study pointed to flow-distortion errors of **similar** magnitude as those in H15.” and suggest that this is an accurate representation based on the above quotes from Huq et al. (2017). As we state in the manuscript, our results can only be used to quantify the sonic anemometer error, if we make assumption on how the different velocity components are affected. Therefore, it is hard to say whether the findings by Huq et al. (2017) agree with our results

The section 6.2, where the Huq et al. (2017) paper is again cited has been reformulated to:
“If we assume that the discrepancy to $4/3$ is due to remaining uncorrected flow distortion and further, that flow distortion affects the observed frequencies equally, which is an assumption supported by the results presented in Huq et al. (2017), the imperfect ratios correspond directly to underestimation in the velocity variances. Since our results do not indicate how each velocity component is affected, it is still difficult to directly use the results presented here to correct the variances. However, some qualitative comparisons can be made. If, for example, the u - and v velocity components are measured with no error, the observed ratios of 1.12–1.19 can only turn into $4/3$ if the w variance is increased by 18–26%, which means that the w component itself should increase by 8–12%. This error range is in agreement with the results by Frank et al. (2016), but higher than the error suggested by Huq et al. (2017). If we, on the other hand, assume equal errors on all velocity components (positive for u and v , and negative for w) the ideal ratio of $4/3$ can be reached with a 4–6% correction on the velocity components. These examples illustrate that our method can be a useful tool for judging whether flow distortion corrections of a particular sonic anemometer are adequate or not, but that it cannot be used directly to quantify the error.” ---

I believe that by addressing these major comments and the following specific comments listed below, that this paper will be appropriate for Atmospheric Measurement Techniques.

Specific comments:

Page 3, line 30: A better definition for “isotropic” should be given before “, which also means”. The assumption of isotropic is critical for the theory that leads to the $4/3$ ratio from which the entire paper is based. So, a clear definition is important.

--- As suggested by the reviewer we have added a description of what isotropy means and

reformulated the sentences regarding local isotropy ---%%%

Page 4, line 1: The statement "...the velocity power spectra follows the relation," is not self-evident to the casual reader. I would recommend clarifying that Kolmogorov determined this.

%%%- We now refer the reader to Pope's 2000 textbook after the equation ---%%%

Page 4, line 5-6: Clarify "outer scale" Does "the most energy containing scales" refer to something similar to the peak of the spectra as shown in figure 1? Is there a way to describe the "Kolmogorov length scale", i.e., when energy dissipation begins?

%%%- Scales are now added to Fig. 1 to clarify the scales in the spectra. We have also added text describing how η can be estimated and that this is much smaller than the sonic path length ---%%%

Figure 1. Could add a $-2/3$ slope reference line for comparison.

%%%- Added as suggested by the reviewer --%%%

Page 5, line 7: Does the component i refer to u , v , or w ?

%%%- See our response to the next comment ---%%%

Page 5, lines 6-15: I found this "crude" description confusing. k_2 and k_3 should be defined. The Φ function should be defined. The sentence on line 15 is a repeat of an earlier statement. My big question is whether or not this section is necessary? I'm not sure it really matters much to the main understanding of the paper why the path averaging correction affects u different than v and w . At least, it might not be important enough to derive the theory behind it.

%%%- We agree with the reviewer. The explanation of the different effects of path averaging on the three velocity components is not essential for the paper and so it is now removed ---%%%

Page 6 line 7 versus Page 7 line 9: Be careful where U is defined as instantaneous versus U defined as an average over 10-minutes.

%%%- U was instantaneous and so to conform also to the definitions in Sect. 2.2.2, we changed " U " in Sect. 2.2.3 to Sh (and call it instantaneous horizontal wind), and replace V by S ---%%%

Table 1: In generally, is there a reason why H06 was only applied to 2 of the 3 datasets? This should be clarified. Also, it is not clear until Table 2 exactly which permutations of the different calculations were analyzed. It wasn't clear from Table 1 and throughout this section which different versions of these data sets were actually tested.

%%%- We now include the possible permutations in Table 1 and in the caption of the table we have added "Due to the height of the instrument at Nørrekær Enge, we did not apply a PA correction as the error should be negligible" ---%%%

Page 8, lines 18 and 23: The terms "quality signal equal to zero" and "no warnings" are confusing. I am assuming these refer to the manufacturer's diagnostic value that comes from the CSAT3.

%%%- We are now consistently referring to the manufacturer's quality signal ---%%%

Page 8, lines 26-30: This is a strange introduction to the results. It is somewhat telling that the results are described as “we show examples”. My intention by encouraging the authors to perform more rigorous statistical analysis (via 1st order polynomial p-values or LOESS regression, etc.) is to make the results less about “examples” and more about rigorous objective metrics. The word “closely” at the end on line 28 implies some sort of goodness of fit test.

%%%--- We have now extended the paragraphs that introduce the results. The sharpened criteria are also firstly described here. See our response to the reviewer’s general comment regarding this issue ---%%%

Page 8, last line on page/Page 9 line1: The first part should probably belong in the methods. For the second part, is this something that was observed from this study, or a more general finding that should have a citation?

%%%--- We have moved some of the lines mentioned by the reviewer to the beginning of Sect. 5 as suggested. As we now state in the same lines, normalization with U is in our study found to reduce the scatter in the velocity spectra ---%%%

Figure 3: Which lines does the “c” plot (i.e., 0th order polynomial) fit, w or v? It probably isn’t u since that is much lower on the graph. On the caption, when it says “perpendicular”, does this mean wind can flow in either direction, e.g., left-right as well as right-left? I assume the range ± 10 deg means the average wind direction, not the range of instantaneous wind direction within the 10-min period?

%%%--- As we have now reformulated the beginning of Sect. 5, it should be clear that the fit is performed on the w spectra. We also added the information in the caption of the figure. Further, we have stated exactly at which relative directions we refer to when saying “parallel” and “perpendicular” in the caption. We now also include in the first paragraph of data treatments that we computed the mean wind direction for each 10-min period and a statement regarding what direction is meant hereafter ---%%%

Page 9, lines 10-12: This might be a vast overreach of the data to assume that because “both intervals” in figure 3 appear to fit within a specific inertial subrange, that it applies “irrespective of the wind conditions”.

%%%--- The paragraph has been rephrased and now we include that this assumption is in fact tested using the sharpened criteria ---%%%

Page 9, second to last sentence: the use of $4/3$ is somewhat misleading here. It really has nothing to do with the $4/3$ in Equation 2. It is purely coincidence that the uncorrected Metek had a w-u ratio of ~ 1 , such that the improvement from uncorrected to corrected increases the value by $\sim 4/3$. To emphasize that this value is not the same as the $4/3$ in equation 2, I would simply state it was a 33% increase.

%%%--- We have changed all instances where $4/3$ is mentioned in relation to the 3D corrected to uncorrected variances and used the suggestion by the reviewer ---%%%

Figure 4. Why is the same graph of w-u red on the left and black on the right? If the running mean was replaced with a LOESS fit, then the confidence interval lines could also be added. In the caption, should clarify if this is the average “wind direction” over the 10-min period.

%%%--- It was not the same graph but we also showed in both frames the 3D corrected w- to u-velocity spectra ratios for a better understanding of the results. However, we now show in right frame the v- to u-velocity spectra ratio for the non- and 3D-corrected data ---%%%

Table 2. The sharpening criteria should be mentioned earlier in the methods. Also, with a 1st-order polynomial/p-value criteria to include only 10-minute periods with no significant deviation from the -5/3 line, then the sharpening criteria would not be necessary.

--- See our response to the general comment regarding the sharpened criteria ---

Page 11, line 18: Does “lower absolute directions” mean “directions more in line with the boom”?

--- We meant low relative directions. We have modified the wording according to the suggestion by the reviewer ---

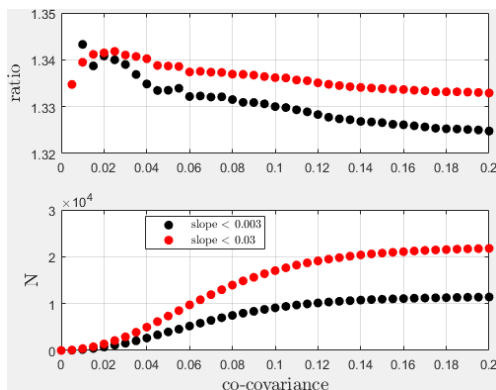
Page 11, line 22: The threshold +/- 0.003 seems arbitrary without some justification. The $F_{uw}/\sqrt{F_u F_w} < 0.02$ criteria should be explained in the methods with the definition of isotropy.

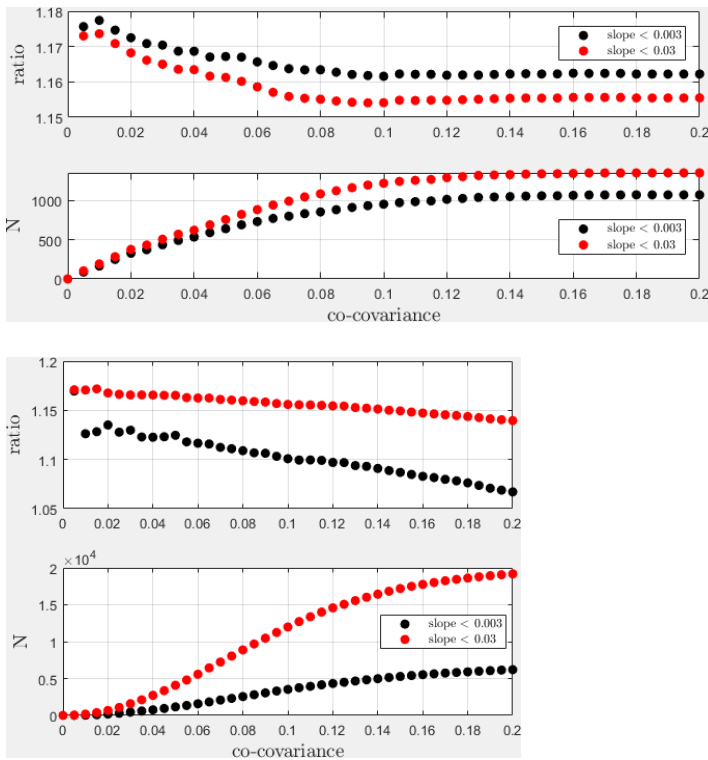
--- The $F_{uw}/\sqrt{F_u F_w}$ criterion, i.e., the uw co-covariance is now moved to the beginning of the results section. As we responded to an earlier comment, the text describing isotropy has been extended and reformulated.

Regarding the choice of thresholds: we have now added the following text to Sect. 6.1 about the uncertainties:

“The choice of thresholds for the sharpened criteria compromised the amount of data left for the analysis; about 4%, 25%, and 1% of the original amount of 10-min periods for the USA-1 at Risø, CSAT3 at Risø and the CSAT3 at Nørrekær Enge, respectively. The choice, however, did not change the velocity spectra ratios significantly. The softening of the values to, e.g., 0.03 and 0.2 for the w -spectral slope and the uw -covariance, respectively, resulted in a change of the w - to u -velocity spectra ratio of $\approx 0.6\%$ for the USA-1, $\approx 1.5\%$ for the CSAT3 at Risø, and $\approx 0.8\%$ for the CSAT3 at Nørrekær Enge, only”

For the reviewer’s interest we have made some graphs showing the sensitivity of the w to u spectra ratios to both thresholds and the results are shown in the next three figures (for the USA-1 at Risø, the CSAT3 at Risø and the CSAT3 at Nørrekær Enge, respectively). The top frame in each plot shows the ratio as a function of the uw co-covariance (x-axis) and two thresholds for the w slope in the inertial subrange. The bottom frame is similar but showing the amount of measurements as function of the thresholds. As illustrated, the ratios at all three sites vary very little when changing these thresholds but the choice was made so that there was still enough data to be analyzed in the case where most observations were filtered out (i.e., Nørrekær Enge).





---%%%

Page 12, line 8: This statement also applies to the Metek, although it is much smaller.

%%-%- We have now a statement regarding this in the USA-1 analysis ---%%%

Page 12, line 19-20: These do not look that much different to me.

%%-%- They might not look that much different but for the CSAT3, the w- to u-spectra at +-180 deg is about 0.3 whereas it is less than 0.2 at Nørrekær Enge ---%%%

Figure 7: There are three different calculation scenarios presented on the right (no correction, H15, H15+H06). Which one of these applies to the left?

%%-%- As noticed by the reviewer, we now include this information in the caption of the figure ---%%%

Page 14, line 19: The presentation of ~ 0.5-1.5% is somewhat confusing. It might be simpler to describe this as “increase by 0.005-0.015”, though by looking at the table this would be “0.008-0.018”.

%%-%- We agree with the reviewer and have rewritten the sentence so that it reads “, which increased the CSAT3 ratios at Risø by 0.6—1.6% only ---%%%

Page 14, line 22: Does this really mean that the sonic was physically rotated? This probably refers to rotating the u, v, and w measurements. Also, this methodology seems overly confusing, when it would be much simpler to reprocess the data with the planar-fit rotation.

%%-%- We understand that a reader could think the anemometer was physically rotated, which was not.

We have therefore changed the sentence to “This was done by rotating the sonic anemometer measurements of the velocity components and applying an isotropic inertial subrange 3D spectral velocity tensor, as in H06, to calculate the nominal component spectra for this configuration.” Our reluctance to use the planar-fit correction stem from earlier results published in Dellwik et al. (2010) ---%%%

Page 15, line 14-15: This assumes that the uncorrected portion of the w measurement is simply a scaling issue.

%%%--- We have reformulated the whole paragraph as we explained in the response to the major comment by the reviewer with regards to our interpretation of the work of Huq et al. (2017) ---%%%

Page 15, line 20-21: I would remove this statement. It is far too oversimplified, and probably extremely unlikely.

%%%--- We find it more unlikely that the error is only on w, and would therefore like to keep the statement in a reformulated version (see our previous response) ---%%%

Page 15, line 27-28: This is a very bold statement, but it may be justified.

%%%--- We have added “, provided that an inertial subrange is clearly apparent” to the sentence ---%%%

Page 15, line 5 (near the bottom): Should clarify “from the corrected USA-1”.

%%%--- Corrected as suggested ---%%%

Page 16, line 26: I am confused about the verb tense. By saying “we propose to perform such an analysis” it reads like a recommendation for future research. That is fine, but if so, a recommendation like this should probably be near the end of the conclusions.

%%%--- Corrected as suggested ---%%%

Page 16, line 30: Similar to an earlier comment, the use of $\sim 4/3$ here is misleading because it does not have anything to do with the $4/3$ in Equation 2. I would use “33% higher than the”.

%%%--- Corrected as suggested ---%%%

References:

Dellwik, E., Mann, J., and Larsen, K. S.: Flow tilt angles near forest edges – Part 1: Sonic anemometry, *Biogeosciences*, 7, 1745-1757, <https://doi.org/10.5194/bg-7-1745-2010>, 2010.

A method to assess the accuracy of sonic anemometer measurements

Alfredo Peña¹, Ebba Dellwik¹, and Jakob Mann¹

¹DTU Wind Energy, Technical University of Denmark, Roskilde, Denmark

Correspondence to: Alfredo Peña (aldi@dtu.dk)

Abstract. We propose a method to assess the accuracy of atmospheric turbulence measurements performed by sonic anemometers and test it by analysis of measurements from two commonly used sonic anemometers, a Metek USA-1 and a Campbell CSAT3, at two locations in Denmark. The method relies on the estimation of the ratio of the vertical to the along-wind velocity power spectrum within the inertial subrange [and does not require the use of another measurement as reference](#). When we correct the USA-1 to account for three-dimensional flow-distortion effects, as recommended by Metek GmbH, the ratio is very close to 4/3 as expected from Kolmogorov's hypothesis, whereas non-corrected data show a ratio close to 1. For the CSAT3, non-corrected data show a ratio close to 1.1 for the two sites and for wind directions where the instrument is not directly affected by the mast. After applying a previously suggested flow-distortion correction, the ratio increases up to ≈ 1.2 , implying that the effect of flow distortion in this instrument is still not properly accounted for.

10 1 Introduction

Accurate observations of atmospheric flow velocities, turbulence, and turbulence fluxes are critical for our understanding of all physical processes that occur in the atmospheric boundary layer and for the improvement of atmospheric modelling. Examples of intensely researched applications of turbulent fluxes include the closure of the surface energy balance (Foken, 2008), as well as the estimation of the carbon balance based on eddy-covariance observations, in which a very small systematic error can have a significant effect on the yearly carbon budget (Ibrom et al., 2007). Other applications include wind-power meteorology: turbulence is an important design parameter for wind turbines as the turbine loads are directly related to the velocity variances and turbulence measurements are therefore needed to find out whether a wind turbine can withstand the local flow conditions (Mücke et al., 2011; Dimitrov et al., 2015).

Our current understanding of atmospheric turbulence is, to a high degree, based on measurements performed with three-dimensional sonic anemometers deployed on meteorological towers. However, sonic anemometer measurements suffer from flow distortion due to the effects of both the structure(s) where the anemometer is mounted on, i.e., booms, clamps, and the bulk of the mast itself (e.g., Dyer, 1981; McCaffrey et al., 2017) and the anemometer itself. The latter effect has been recognized as a limitation for the accuracy of sonic anemometer observations for several decades (Wyngaard, 1981; Zhang et al., 1986; Grelle and Lindroth, 1994; van der Molen et al., 2004; Horst et al., 2015).

Some of the first wind-tunnel investigations on how the sonic anemometer structure impacts the measurements' accuracy were performed on the Kaijo-Denki DAT-300 sonic anemometer (Kraan and Oost, 1989; Mortensen, 1994). They showed

azimuth-dependent errors in the observed wind speed, which reflected the geometry of the probe head. These studies were followed by wind-tunnel investigations of the much more slender Gill R2 sonic anemometers by Grelle and Lindroth (1994), who showed the influence from the three supporting bars on the probe head leading to maximum wind speed errors of 15%, whereas the change of tilt within a small interval of angles showed less effect. This study was followed by that of Mortensen and Højstrup (1995), who showed influence on the accuracy of the measured velocity both from the ambient temperature and wind speed. Later, van der Molen et al. (2004) investigated Gill R2 and R3 sonic anemometers for a much wider range of tilt angles than those from the previous two studies. They demonstrated that the vertical velocity was severely underestimated at large tilt angles. Whereas surface sensible heat flux observations taken over forest increased by 4% using the calibration scheme by Grelle and Lindroth (1994), the calibration scheme by van der Molen et al. (2004) resulted in sensible heat flux increases of 15% for a different forested site. For the USA-1 (or its more modern version the uSonic3) sonic anemometer from Metek GmbH, Hamburg, Germany, two-dimensional and three-dimensional flow-distortion corrections were provided by Metek GmbH (2004) (hereafter M04). They are based on wind-tunnel observations for a number of azimuths and tilt angles.

Högström and Smedman (2004) documented an intercomparison between hot-film anemometers and Gill Solent R2 and R3 sonic anemometers. Both types of instruments were calibrated in a wind tunnel and subsequently intercompared in full-scale experiments. Whereas the hot-film anemometers retained their precision from the calibration, that of the sonic anemometers deteriorated in the field tests. Högström and Smedman (2004) argued that this difference could be explained by the effect of atmospheric turbulence and, hence, that wind-tunnel-based calibrations may therefore not be valid.

Another method for testing the precision and accuracy of sonic anemometers is to mount different brands closely and study the agreement between their turbulence measurements (e.g., Mauder et al., 2007; Kochendorfer et al., 2012). The challenge with this method is the difficulty to objectively determine which of the sonic anemometers measures best. Also, if agreement is found, this could be due to a similar error.

A third variant for assessing sonic anemometer performance is by comparing ~~some~~ several of the same brand, by mounting them at different tilts ~~and azimuths~~ (Meyers and Heuer, 2006; Kochendorfer et al., 2012; Nakai and Shimoyama, 2012) and azimuths (Kaimal et al., 1990). Nakai and Shimoyama (2012) used five Wind-Master sonic anemometers mounted at different angles relative to each other and deduced flow distortion correction schemes based on the anemometers' different response as a function of both tilt and azimuth angles. Since the geometry of the Wind-Master is identical to that of the Solent R2 and R3, the resulting flow-distortion correction scheme could be compared to that of van der Molen et al. (2004). The new scheme by Nakai and Shimoyama (2012) pointed to slightly higher increases in the turbulent fluxes than that by van der Molen et al. (2004). Kochendorfer et al. (2012) used three sonic anemometers by R. M. Young, and studied the observations of the vertical wind speed over a wide range of azimuth and tilt angles. They found that for their sites, the vertical wind speed was underestimated by $\approx 11\%$, and when applying their derived corrections, the heat fluxes increased by 9–13%. Whereas this method avoids the potential problems associated with quasi-laminar wind-tunnel calibrations, the accuracy of the correction cannot be better than the accuracy of the instrument chosen as the reference. Also, it is hard to evaluate whether the somewhat "busy" setup with several sonic anemometers in a small area ~~can~~ could lead to additional and larger flow distortions than those using a single sonic anemometer.

Several combinations of the three different methods outlined above (*i* wind-tunnel calibration, *ii* comparison of different brands of sonic anemometers, and *iii* tilting sonic anemometers of the same brand relative to each other) have also been demonstrated. Kochendorfer et al. (2012) used two sonic anemometers by R. M. Young and an orthogonal sonic anemometer by ATI as reference, and studied the observations of the vertical wind speed over a wide range of azimuth and tilt angles. They found that for their sites, the vertical wind speed was underestimated by $\approx 11\%$, and when applying their derived corrections, the heat fluxes increased by 9–13%. A similar setup was used by Frank et al. (2013), who also used four CSAT3 and one ATI sonic anemometer, where two of the CSAT3 instruments were rotated 90° . Frank et al. (2013) showed that the CSAT3 sonic anemometer by Campbell, Logan, US, underestimated the vertical velocities and that this, which led to an underestimation of the sensible heat flux of about 10%. Horst et al. (2015) (hereafter H15) used a combination of all the three methods to derive a flow distortion correction for the CSAT3. Their correction, when applied to sensible heat flux data taken over an orchard canopy, showed a more modest effect closer to 5%. Based on the same data as those in Frank et al. (2013), Frank et al. (2016) demonstrated the use of a Bayesian model to estimate the most likely flow-distortion correction scheme of the CSAT3 and found a 10% increase in vertical velocities and sensible heat flux as well. Huq et al. (2017) presented a novel approach for estimating the accuracy of the CSAT3 by using numerical simulations. The results of the study pointed to flow-distortion errors of similar magnitude as those in H15. The discrepancies in the findings of the previous studies foster the debate on the magnitude of the CSAT3 flow-distortion correction. Given the key role that sonic anemometers have in the field of experimental micrometeorology, it is of great importance to find objective standards by which accuracy and precision can be evaluated.

The aim of the current study is two-fold. First we introduce a new reference method for evaluating sonic anemometer accuracy, and second, we evaluate the effect of flow-distortion corrections for two different sonic anemometers using this reference method. The two sonic anemometers are the USA-1, for which we apply the manufacturer's flow-distortion correction, which is based on wind-tunnel measurements, and the CSAT3, for which we apply the correction by H15. To our knowledge, the reference method, which is simply based on the relation between the velocity spectra within the inertial subrange, has not been used previously for diagnosing sonic anemometer accuracy.

2 Background and methods

We first start by introducing the expected relations between velocity spectra within the inertial subrange in Sect. 2.1 and later introduce the flow corrections commonly used for sonic anemometers measurements in Sect. 2.2.

2.1 Inertial subrange

The inertial subrange corresponds to the region in the atmospheric energy spectrum where energy is neither produced nor dissipated, and where the transfer of energy from the energy containing range (buoyancy- and shear-produced energy) to the dissipation range (kinetic to internal energy) is controlled by ε , which is the rate at which energy is converted to heat in the dissipation range (Kaimal and Finnigan, 1994).

Following the dimensional considerations of Kolmogorov (1941), the power spectrum of u , which is that of the along-wind component of the velocity, within the inertial subrange becomes

$$F_u(k_1) = \alpha \varepsilon^{2/3} k_1^{-5/3}, \quad (1)$$

where k_1 is the along-wind wavenumber and α is the universal Kolmogorov constant (≈ 0.5). ~~Turbulence is Statistical isotropy of the second-order means that any second-order statistics does not change if the coordinate system is rotated in any way. This would imply that the variances of the three velocity components would be identical and the co-variances would be zero. But we can say that turbulence is~~ locally isotropic within ~~this range, which also means that the inertial subrange, which means that beyond that wavenumber all one-point~~ correlations between velocity components become zero. ~~cross-spectra between different velocity components approach zero. For example, the cross-spectrum between u and w decreases like $k_1^{-7/3}$, which is more rapid than F_u and the bulk of the momentum flux $\langle u'w' \rangle$, where the prime indicates fluctuations, is located at a wavenumber lower than the inertial subrange.~~ Due to incompressibility and isotropy, the velocity power spectra follows the relation ~~(Pope, 2000),~~

$$F_{uw}(k_1) = \frac{3}{4} F_v(k_1) = \frac{3}{4} \frac{4}{3} F_{wu}(k_1), \quad (2)$$

where v and w are the cross and vertical velocity components, respectively. Figure 1 illustrates idealized velocity spectra showing the spectral regions, the behavior of each velocity component, and the relations in the inertial subrange. It is important to note that Eqn. (2) is only an asymptotic relation valid for $1/L \ll k_1 \ll 1/\eta$ where L is an outer scale of the turbulence, for example, the most energy containing scales, and $\eta = (\nu^3/\varepsilon)^{1/4}$, where η is the Kolmogorov length scale ~~and ν the kinematic viscosity. Also important is that η is much smaller than the distance between transducers of a typical sonic anemometer (also known as path length), so viscosity is not important for the fluctuations measured by such an instrument.~~

2.2 Corrections to sonic anemometer measurements

2.2.1 Path-length averaging correction

For observations taken near the surface, or during stable atmospheric conditions, the ~~distance between the sonic anemometer transducers (the path length p)~~ over which the wind field is averaged may be a significant fraction of the length scale of the turbulence. A measured velocity power spectrum can therefore show a reduction of magnitude in the inertial subrange. Using similar methods as in Kaimal et al. (1968), Horst and Oncley (2006) (hereafter H06) calculated how path-length averaging influences sonic anemometer measurements for the geometries of the CSAT3 and Gill R3 sonic anemometers. The path-length averaging errors are expressed as transfer functions for each velocity component and depend on $k_1 p$. Here, we implement the results by H06 using the transfer functions for each of the velocity components by means of interpolation of tabular values to observed $k_1 p$ values. The tabular values for the CSAT3 are listed in H06, Table BI, Appendix B. Since the USA-1 has the same geometry as the Gill R3, the values in Table BII, Appendix B in H06 can be applied to the former instrument. It turns out that the effect of path-length averaging on the three velocity components is different for both the CSAT3 and Gill R3

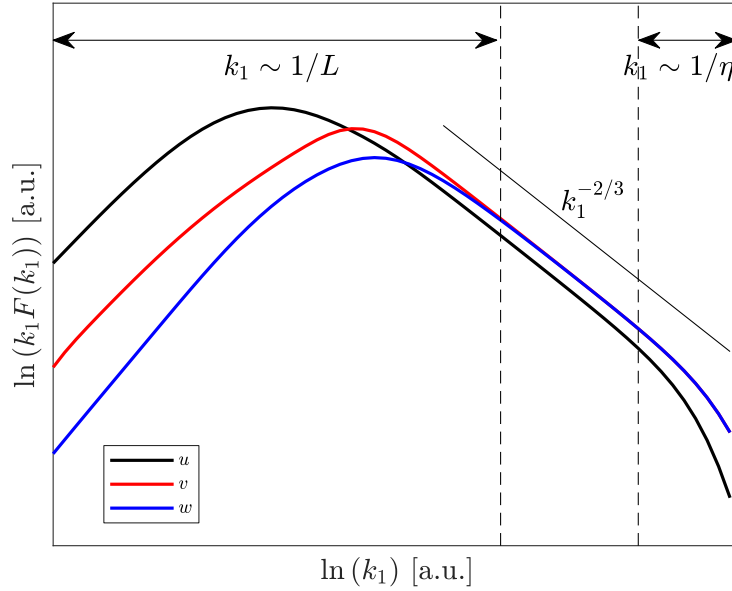


Figure 1. Idealized atmospheric velocity spectra showing the spectral regions and the relations in the inertial subrange (indicated within the vertical dashed lines). Notice that the spectra in the y -axis are premultiplied by k_1 and so the spectral slope is $-2/3$ instead of $-5/3$ as in Eqn. (1)

geometries. For $k_1 < 1/p$, which is the most relevant range for this investigation, the u -component is more attenuated than the v - and w -components. This can crudely be understood by taking into account the incompressibility of the flow. For any given component i , the one-dimensional spectrum can be expressed by adding all the three-dimensional spectral densities with the same k_1 :

$$5 \quad F_i(k_1) = \int_{-\infty}^{\infty} \int_{-\infty}^{\infty} \Phi_{ii}(k_1, k_2, k_3) dk_2 dk_3$$

where we follow the notation of H06. The majority of the energy for the v - and w -components comes in the inertial subrange from the three-dimensional spectral densities with the smallest magnitude of $\mathbf{k} = (k_1, k_2, k_3)$, i.e., when k_2 and k_3 are close to zero and $k \equiv |\mathbf{k}| \approx k_1$. However, for the u -component, $\Phi_{11}(k_1, 0, 0) = 0$ because of incompressibility, so the bulk of $F_1(k_1)$ comes from $\Phi_{11}(\mathbf{k})$ where k_2 or k_3 are far from zero. In these situations $k > k_1$, so the three-dimensional Fourier components contributing to the one-dimensional spectrum have shorter wavelengths. In general, shorter wavelengths mean that the effect of averaging becomes stronger, thus we can expect the attenuation of the u -component to be strongest, at least for $k_1 < 1/p$.

2.2.2 Flow-distortion correction for the CSAT3 sonic anemometer

We implement the scheme by H15, which is based on that by Wyngaard and Zhang (1985) and calibrated through wind tunnel observations. The procedure follows:

1. Calculation of the length of the instantaneous wind vector $S = \sqrt{x^2 + y^2 + z^2}$, where x , y , and z are the raw velocity components in the instrument's coordinate system.
2. Projection of the velocity components $\mathbf{u} = (x, y, z)$ to the vectors defined by the paths of the sonic anemometer.
3. Calculation of the angle between the wind vector and each of the paths (subindex p), $\theta_i = \arccos(u_{p,i}/S)$, where $i = 1-3$ denote paths 1-3, and $u_{p,i}$ the projection of the velocity component on each path.
4. Correction (subindex c) of transducer shadowing $u_{p,i,c} = u_{p,i}/(0.84 + 0.16 \sin \theta_i)$.
5. A final rotation of the corrected velocities back to a Cartesian coordinate system.

2.2.3 Flow distortion corrections for the Metek USA-1 sonic anemometer

There are two types of flow corrections available for the USA-1. The first one is a two-dimensional (2D) correction that takes into account the azimuth angle and, the second, a three-dimensional (3D) correction accounting for the tilt as well. Both are suggested by M04. The 2D-corrected velocities are

$$x_{2D} = x\delta, \quad (3)$$

$$y_{2D} = y\delta, \quad (4)$$

$$z_{2D} = z + 0.031U_r [\sin(3\alpha) - 1], \quad (5)$$

where $\delta = 1.00 + 0.015 \sin(3\alpha + \pi/6)$, $U_r = \delta (x^2 + y^2)^{1/2}$, and $\alpha = -\text{atan2}(y, x)$. The 3D correction is applied through lookup tables (LUTs) derived from wind-tunnel measurements. Defining the ~~horizontal and total velocity as $U = (x^2 + y^2)^{1/2}$ instantaneous horizontal wind vector as $S_h = (x^2 + y^2)^{1/2}$~~ and ~~$V = (x^2 + y^2 + z^2)^{1/2}$, respectively, and~~ the azimuth and tilt angles as $\alpha = \text{atan2}(-y, -x)$ and ~~$\phi = -\text{atan2}(z, U)$~~ ~~$\phi = -\text{atan2}(z, S_h)$~~ , the velocity, azimuth, and tilt are corrected as,

$$V_{3D} = n_c(\alpha, \phi) \underline{V} \underline{S}, \quad (6)$$

$$\alpha_{3D} = \alpha + \alpha_c(\alpha, \phi), \quad (7)$$

$$\phi_{3D} = \phi + \phi_c(\alpha, \phi), \quad (8)$$

where $n_c(\alpha, \phi)$, $\alpha_c(\alpha, \phi)$, and $\phi_c(\alpha, \phi)$ are α - and ϕ -dependent correction factors¹, which are computed through Fourier series with coefficients $C_{f_c,i}(\phi)$ and $S_{f_c,i}(\phi)$ that are provided in the LUTs,

$$f_c(\alpha, \phi) = \sum_{i=0,3,6,9} [C_{f_c,i}(\phi) \cos(i\alpha) + S_{f_c,i}(\phi) \sin(i\alpha)], \quad (9)$$

¹note that there is a typo in V_{3D} in M04

where $f_c(\alpha, \phi)$ is either $n_c(\alpha, \phi)$, $\alpha_c(\alpha, \phi)$, or $\phi_c(\alpha, \phi)$. The LUTs are not given in M04 and so we provide them in Appendix A. The 3D-corrected velocities are,

$$x_{3D} = -V_{3D} \cos \alpha_{3D} \cos \phi_{3D}, \quad (10)$$

$$y_{3D} = -V_{3D} \sin \alpha_{3D} \cos \phi_{3D}, \quad (11)$$

$$5 \quad z_{3D} = -V_{3D} \sin \phi_{3D}. \quad (12)$$

3 Sites and instrumentation

Measurements ~~are~~ were collected from sonic anemometers mounted on three meteorological masts at two sites in Denmark: the Risø test site on the Zealand island and the Nørrekær Enge wind farm on northern Jutland (see Fig. 2). The Risø test site is over a slightly undulating terrain with a mix of cropland, grassland, artificial land, and coast (the Roskilde Fjord coastline is ≈ 250 m northwest of the turbine stands). The Nørrekær Enge wind farm is located ≈ 350 m southeast of the water body Limfjorden over flat terrain with a mix of croplands and grasslands.

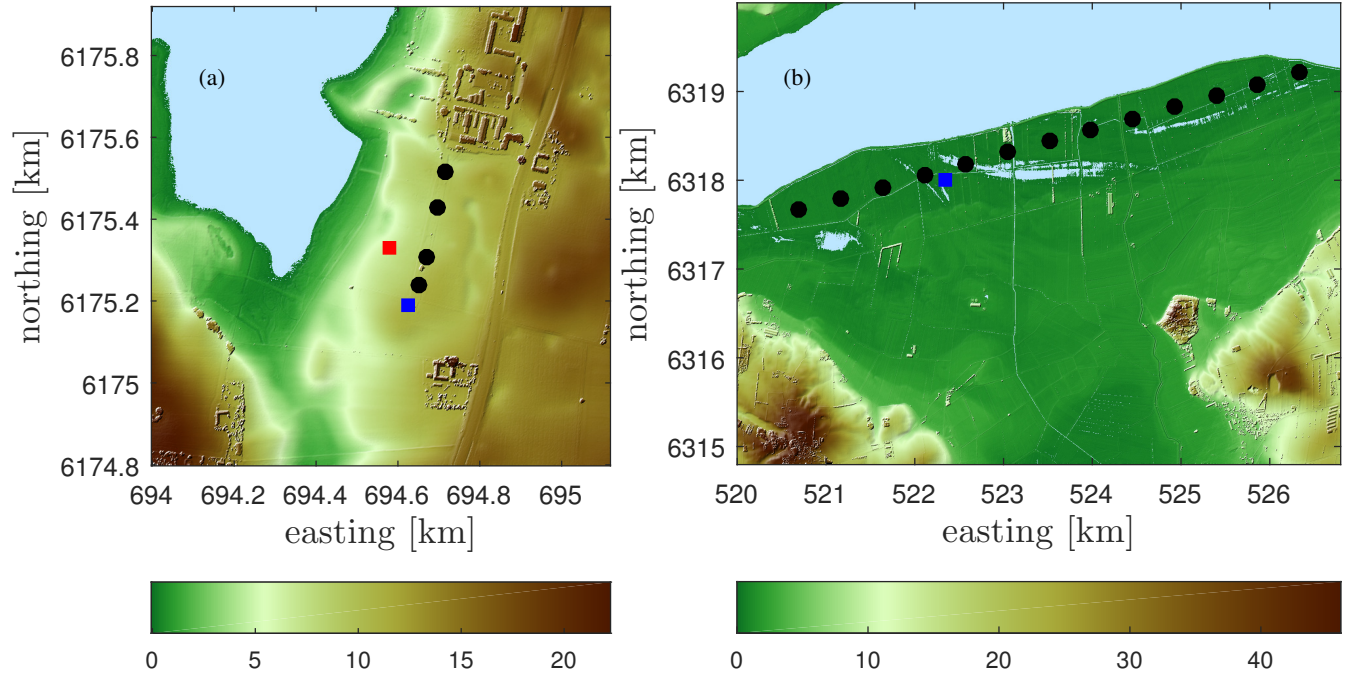


Figure 2. Locations of the sonic anemometer measurements. Wind turbines are indicated in black circles, masts with a CSAT3 on blue squares, and the mast with a USA-1 in a red square. ~~The left panel~~ Panel (a) shows the Risø test site and ~~(b) the right panel~~ the Nørrekær wind farm site. The colorbar indicates the height above mean sea level in meters based on a digital surface elevation model (UTM32 WGS84)

At the Risø test site, a CSAT3 was mounted at 6.4 m above ground level (agl) on a 2.5-m boom on a 15-m tall tower. The boom was oriented 14° from the north. The tower was a triangular lattice structure with a side length of 0.4 m at the

measurement height. The data acquisition unit was placed on the western leg of the tower, just below the boom. From the point of view of the mast, turbines were located within the direction sector 16–29°.

Also at the Risø test site, but on a different mast, a USA-1 Basic was mounted at 16.5 m agl on a 2-m boom, which is oriented ~~15~~10° from the north, on a 54-m tall tower that is located west of the wind turbine stands. The tower is a square lattice structure 0.3 m wide from bottom to top. From the point of view of the mast, turbines are located within the direction sector 36–142°.

At the Nørrekær Enge wind farm, a CSAT3 was mounted at 76 m agl on a 3.1-m boom, which is oriented 192.5° from the north, on a 80-m mast that is located southeast of the row of wind turbines between stands 4 and 5 (numbered from left to right). From the point of view of the mast, these two turbines are located within the direction sector 281–40°. The closest turbine (4) is at 232 m and turbines are separated by 487 m. The mast is an equilateral triangular lattice structure with a width of 0.4 m at 80 m.

At all sites the sonic anemometers were mounted so that their north was aligned with the boom direction. Thus, wind directions are hereafter relative to the sonic anemometer orientation where 0° is aligned with the boom. In Table 1, the specifications of the sonic anemometers at the two sites and the applied corrections are provided.

Table 1. Sonic anemometer specifications for each measurement site including the ~~use-types~~ of flow distortion (FD) and/or path averaging (PA) corrections applied. Due to the height of the instrument at Nørrekær Enge, we did not apply a PA correction as the error should be negligible

site	sonic anemometer	height agl [m]	p [mm]	type-types of correction
Risø	USA-1	16.5	175	<u>none</u> <u>FD (M04)</u> PA (H06) and FD (M04)
Risø	CSAT3	6.4	115	<u>none</u> <u>FD(H15)</u> PA (H06) and FD (H15)
Nørrekær Enge	CSAT3	76.0	115	<u>none</u> FD (H15)

15 4 Data treatments

For all sonic anemometers, we ~~analyze-analyzed~~ the time series of the three velocity components on a 10-min basis when $U > 3 \text{ m s}^{-1}$. We ~~apply-applied~~ azimuth and tilt rotations to the time series so that u ~~becomes-became~~ aligned with the mean wind vector for each 10-min period. Finally, we ~~compute-computed~~ all velocity spectra and co-spectra as well as the mean wind direction for each 10-min period. All mentions to ‘direction’ are hereafter refer to the 10-min mean relative to the boom orientation.

4.1 USA-1 at the Risø test site

The USA-1 measurements at Risø were sampled at 20 Hz. We ~~use~~used 25401 10-min time series of measurements conducted in 2014 in order to have sufficient data covering all directions. We ~~do~~did all spectra calculations on both the raw (non-corrected data), the 2D- and 3D-corrected data. We also ~~apply~~applied the path-length averaging correction by H06 to the 3D-corrected data.

4.2 CSAT3 at the Risø test site

The CSAT3 measurements at Risø were taken between November 2013 and mid-January 2014, and sampled at 60 Hz. For the analysis, it was required that all recorded velocities had ~~a~~the manufacturer's quality signal equal to zero. Two velocity corrections ~~are~~were performed, the path-length averaging (H06) and the flow-distortion correction suggested by H15. After ~~filtering for no quality warnings~~the quality signal filter, the amount of 10-min time series left ~~are~~were 2720.

4.3 CSAT3 at the Nørrekær Enge wind farm

The CSAT3 measurements at Nørrekær Enge were sampled at 10 Hz. We ~~use~~used 27837 10-min time series of measurements conducted in 2015, when ~~no warnings were recorded by the CSAT3~~the manufacturer's quality signal was equal to zero and no precipitation was recorded by a rain gauge on the mast. We also ~~apply~~applied the flow-distortion correction suggested by H15.

5 Results

For the three sonic anemometers, we ~~show examples of first~~show velocity spectra ensemble-averaged over ~~specific wind direction intervals. This is done to~~two direction intervals, one parallel and another perpendicular to the boom direction. The wavenumber premultiplied spectra was normalized using the horizontal wind-speed magnitude, which, in our analysis, has been shown to reduce the scatter in the velocity spectra. To illustrate that within ~~the chosen a~~a wavenumber range, the velocity spectra ratios approach the theoretical spectral slopes of the inertial subrange closely~~-, the wavenumber premultiplied spectra was multiplied by $k_1^{2/3}$ (in contrast to the idealized wavenumber premultiplied spectra in Fig. 1) so that the inertial subrange can be distinguished as a flat region.~~

Second, for the selected wavenumber range, the velocity spectra ratios were computed for each 10-min sample and the statistics of these ratios were calculated for a wind direction range where the influence of the mast should be the lowest and incorporated in Table 2. We also show all 10-min velocity spectra ratios as function of direction (with and without flow corrections). For the specific case of the USA-1, we show the ratios of the velocity variances as function of direction as well.

Further, to assess whether or not within the selected wavenumber range the velocity spectra conformed to the expected behavior within the inertial subrange, we also filtered out 'poorly' behaved spectra (e.g., from those wind turbine wake affected winds) by assuring that within the selected wavenumber range, both the slope of the w -velocity spectrum was $-5/3 \pm 0.003$ and $|F_{uw}/\sqrt{F_u F_w}| < 0.02$ (i.e., a uw -co-covariance test narrowing for isotropy, see Sect. 2.1) for each 10-min sample. The

slope was computed by fitting a 0-degree polynomial to the normalized w -spectra within the selected wavenumber range. We call these two latter tests 'sharpened' criteria in Table 2.

5.1 USA-1 at the Risø test site

Figure 3 shows two examples of 3D-corrected velocity spectra, ensemble-averaged over two direction intervals for measurements of the USA-1 at the Risø test site. ~~The spectra are normalized using the horizontal wind speed magnitude, which is found to be a better scaling factor than any velocity variance or co-variance in terms of data scatter, and are multiplied by $k_1^{2/3}$ so that the inertial subrange can be distinguished as a flat region. To such normalized spectra, we fit a 0-degree polynomial within a wavenumber range to show that within this range the spectra are indeed flat.~~

Ensemble-average 3D-corrected velocity spectra by the USA-1 at the Risø test site at 16.5 m for two directions intervals: one parallel (left panel) and another perpendicular (right panel) to the boom ± 10 deg. A 0-degree polynomial (c) is fit to the wavenumber range indicated in black vertical lines

It is seen that for both direction intervals, the region in which the w -velocity spectrum becomes flat, is within the same wavenumber range ($0.5 \text{ m}^{-1} \leq k_1 \leq 1.8 \text{ m}^{-1}$). ~~Thus, each 10-min spectrum can be analyzed within the same range, irrespective of the wind conditions.~~ It is also observed that the spectra of the directions parallel to the sonic orientation have higher power spectral density than those of the directions perpendicular because for the latter the spectra are influenced by the fjord. Thus, we assumed at first that each 10-min spectrum can be analyzed within the same range, irrespective of the wind conditions; this assumption is later tested using the sharpened criteria.

Figure 4-left

Figure 4a shows the w - to u -spectra ratio for each non-corrected and 3D-corrected 10 min. It is clearly seen that the non-corrected data approach a ratio close to one, whereas the 3D-corrected data approach 4/3. ~~Figure 4-right shows the 3D-corrected results for both the w - to u - and the v - to u -spectra ratios.~~ Figure 4-right shows the 3D-corrected results for both the w - to u - and the v - to u -spectra ratios. It is also observed that for the latter the data also approach a ratio close to 4/3. 3, although the 3D correction seems to generally increase the ratio. u - and v -spectra ~~do did~~ not change much after the 3D correction (not shown). Table 2 provides the computed velocity spectra ratios within the inertial subrange, for the direction interval where ~~there is was~~ no direct influence by the mast or winds were not affected by turbine wakes, and for both the non-corrected measurements, the 3D corrected, and the path-length averaging- and 3D-corrected measurements. It is important to note that for all correction types, the v - to u -spectra ratio is close to 4/3 and that by applying the sharpened criteria, the statistics on both spectra ratios did not change significantly. The effect of path-length averaging (H06) on the spectra ratios was opposite to that of the 3D correction but rather small.

Figure 5 shows the ratio of the 3D-corrected to the non-corrected velocity variances as function of wind direction. It is clearly seen that the 3D correction ~~does did~~ not only change the spectral density of w within the inertial subrange but that it ~~increases increased~~ the spectral density at all wavenumbers, and so the 3D-corrected variance is ~~4/3 33.33% higher than~~ the non-corrected one. As expected, the 3D correction ~~does did~~ not change the u - and v -variances much.

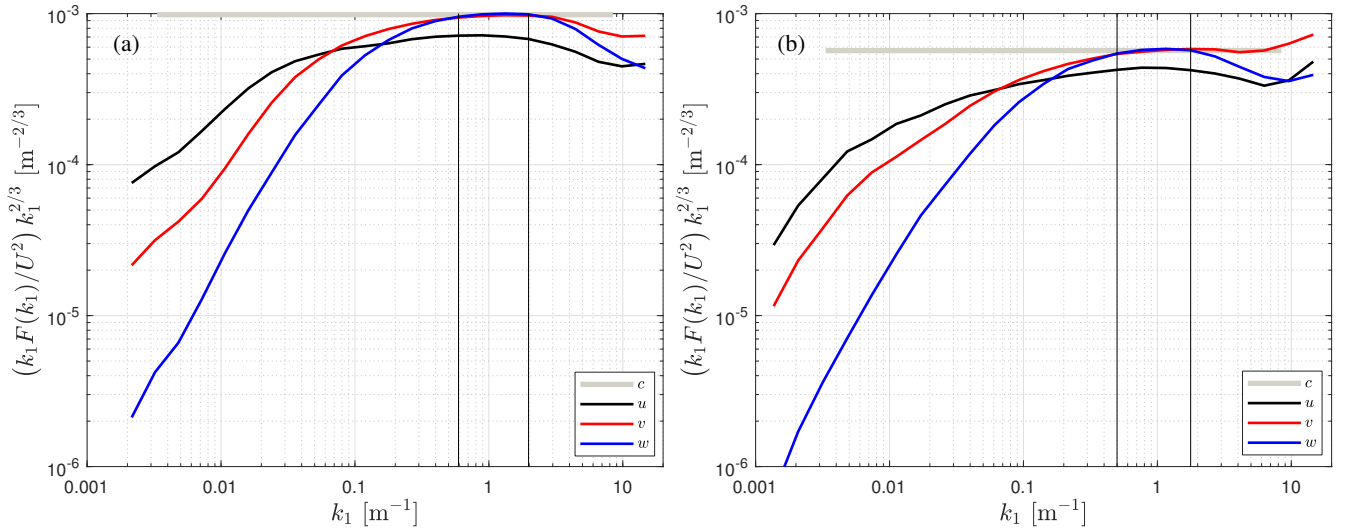


Figure 3. Ensemble-average 3D-corrected velocity spectra by the USA-1 at the Risø test site at 16.5 m for two directions intervals: one parallel 0 ± 10 deg (a) and another perpendicular 90 ± 10 deg (b) to the boom. A 0-degree polynomial (c) was fit to the normalized w -spectra within the wavenumber range indicated in black vertical lines

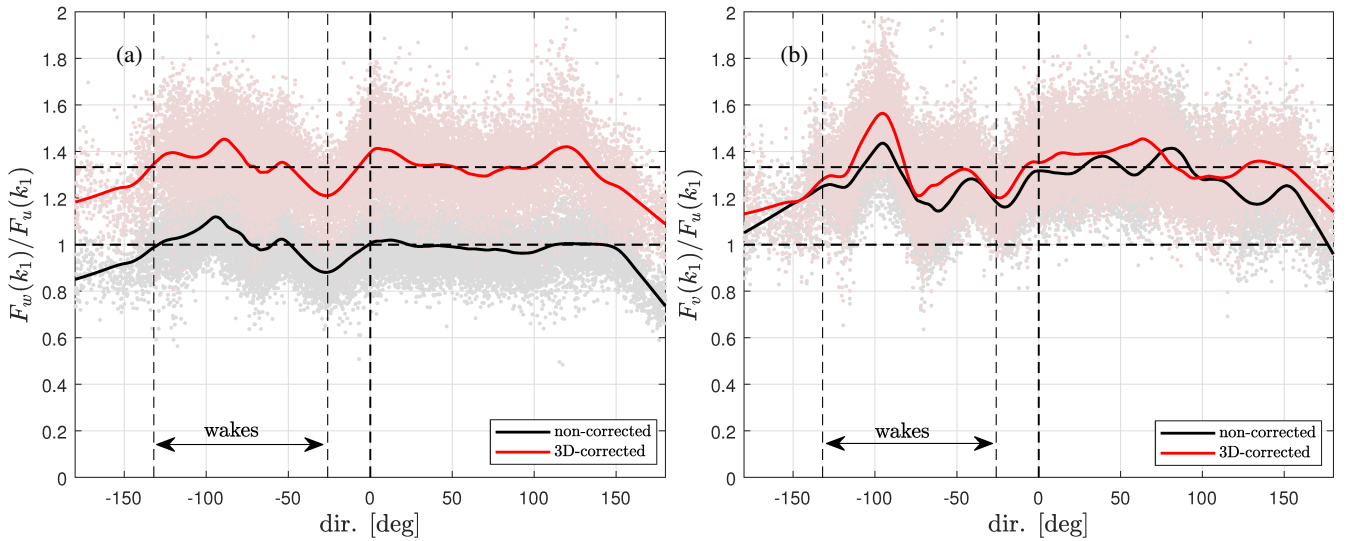


Figure 4. Velocity spectra ratios by the USA-1 at the Risø test site as function of wind direction. (Left frame) w - to u -velocity spectra ratio for the non- and 3D-corrected data. (Right frame) w - and v - to u -velocity spectra ratios for the non- and 3D-corrected data. Each 10-min ratio is shown in markers and the solid lines show a moving average loess fit of the scatter. The thick dashed vertical line indicates the 0° direction, the thin dashed vertical lines indicate the sector with possible turbine wakes, and two dashed horizontal lines indicate the values 1 and $4/33$. The standard error of the fit to the 3D-corrected w - to u -velocity spectra ratios is within 0.0020–0.0031

Table 2. Computed velocity spectra ratios within the inertial subrange for the direction range within ± 120 deg and excluding directions possibly affected by turbine wakes. The mean value is given \pm one standard deviation.

site	sonic anemometer	correction type	sharpened criteria	$F_w(k_1)/F_u(k_1)$	$F_v(k_1)/F_u(k_1)$
Risø	USA-1	none	no	0.999 ± 0.097 0.984 ± 0.089	1.283 ± 0.139 1.322 ± 0.135
Risø	USA-1	FD (M04)	no	1.348 ± 0.128 1.343 ± 0.125	1.345 ± 0.145 1.362 ± 0.135
Risø	USA-1	FD (M04) and PA (H06)	no	1.333 ± 0.125 1.328 ± 0.124	1.332 ± 0.145 1.346 ± 0.135
<u>Risø</u>	<u>USA-1</u>	<u>FD (M04) and PA (H06)</u>	<u>yes</u>	1.336 ± 0.123	1.354 ± 0.135
Risø	CSAT3	none	no	1.132 ± 0.065	1.344 ± 0.091
Risø	CSAT3	FD (H15)	no	1.194 ± 0.070	1.373 ± 0.093
Risø	CSAT3	FD (H15) and PA (H06)	no	1.155 ± 0.068	1.320 ± 0.089
Risø	CSAT3	FD (H15) and PA (H06)	yes	1.163 ± 0.070 1.173 ± 0.070	1.314 ± 0.087 1.312 ± 0.087
Nørrekær Enge	CSAT3	none	no	1.061 ± 0.217 1.070 ± 0.220	1.319 ± 0.315 1.319 ± 0.315
Nørrekær Enge	CSAT3	FD (H15)	no	1.117 ± 0.234 1.127 ± 0.237	1.339 ± 0.331 1.340 ± 0.331
Nørrekær Enge	CSAT3	FD (H15)	yes	1.135 ± 0.235 1.162 ± 0.213	1.317 ± 0.178 1.323 ± 0.178

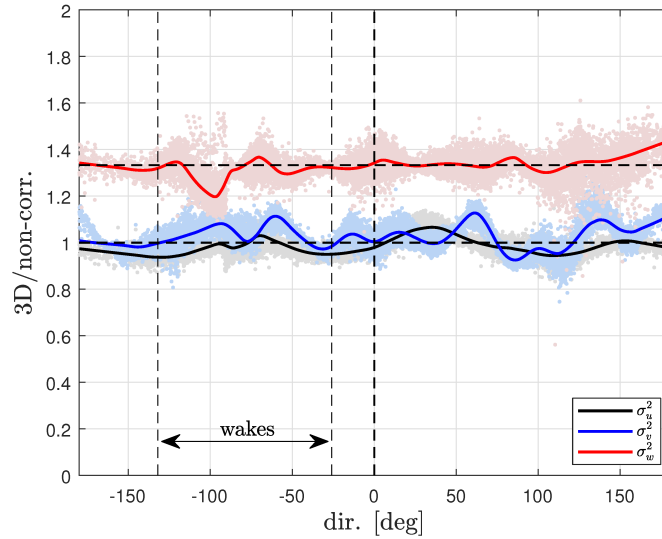


Figure 5. Ratios of the 3D-corrected to the non-corrected velocity variances by the USA-1 at the Risø test site as function of the wind direction. Each 10-min ratio is shown in markers and the lines show a moving average of the scatter. Horizontal and vertical dashed lines as in Fig. 4

5.2 CSAT3 at the Risø test site

From the investigated sonic anemometers, the CSAT3 at Risø had the lowest measurement height. Since the velocity spectra scale with height, the inertial subrange is was expected to be within a range of higher wavenumbers compared to those from the other two sonic anemometers. The wavenumber range at which the premultiplied velocity spectra from this sonic anemometer shows showed an approximately flat range is $k_1 = [2, 5] \text{ m}^{-1}$ (see Fig. 6). Such high wave numbers may might be affected by white noise from the data acquisition itself. The upper limit of the k_1 interval chosen for analysis is was therefore limited, particularly for the u and v components (refer to Appendix B for an explanation of why each velocity component is affected differently by noise), which causes caused the spectral slope to be greater than $-5/3$. $-5/3$.

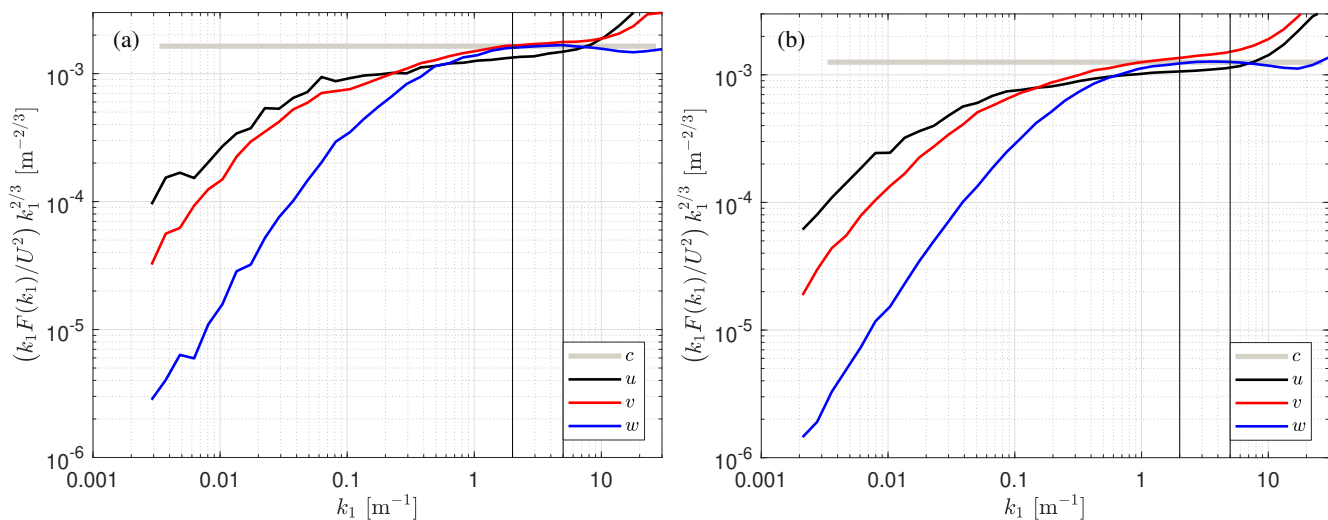


Figure 6. Similar to Fig. 3, but for the CSAT3 at the Risø test site. For the direction parallel to the boom $\pm 10^\circ$ (left frame), the average spectra is was computed over 72 10-min samples, whereas for the directions perpendicular to the boom $\pm 10^\circ$ (right frame), the average is was based on 453 10-min samples

~~For the selected wavenumber range, the ratios are computed for each 10-min sample.~~ Figure 7 illustrates the computed velocity-component spectra ratios. Both $F_w(k_1)/F_u(k_1)$ and $F_v(k_1)/F_u(k_1)$ show showed very low values for absolute directions greater than ≈ 150 deg. For lower absolute directions directions more aligned to the boom, the ratios vary varied between 1.0 and 1.6 (Fig 7-left). For most of the directional intervals, the ratio $F_v(k_1)/F_u(k_1)$ is was clearly higher than the $F_w(k_1)/F_u(k_1)$ ratio. ~~To understand whether the data spread is due to incorrect choice of spectral range, in which perfect inertial-subrange behavior cannot be expected, we sharpen the selection criteria, i.e., we try to filter out ‘poor’ spectra, by assuring that within the selected wavenumber range both the spectral slope is $-5/3 \pm 0.003$ and $|F_{uw}/\sqrt{F_u F_w}| < 0.02$ (i.e., narrowing for isotropy). However, as shown~~ Due to the large difference in heights between this sonic anemometer and the hub height of the turbines in the site and because the closest turbine to the mast was not in operation during the acquisition of the sonic anemometer measurements, we judged that the wake effects are negligible for the computed ratios in Table 2. As shown

in the table, the results for the mean velocity ratios ~~are were~~ insensitive to the poor spectra filter. As for the USA-1 at Risø, for all correction types and criteria used, the v - to u -spectra ratio was close to $4/3$.

In Fig. 7-right**b**, we show the ~~mean of the spectra ratio over each 5° interval for three loess fit for the~~ cases: no correction, H15 correction, and combining the H06 and H15 corrections. Whereas the H15 correction ~~increases increased~~ the ratios, by adding the H06 correction the ratio ~~is was~~ reduced. It can be observed that the effect of path-length averaging (H06) ~~is was~~ opposite to that of transducer shadowing (H15). As discussed before, F_u is attenuated more than F_v and F_w by path-length averaging in the inertial subrange. Therefore, when path-length averaging ~~is was~~ accounted for, the ratios ~~reduced reduced~~.

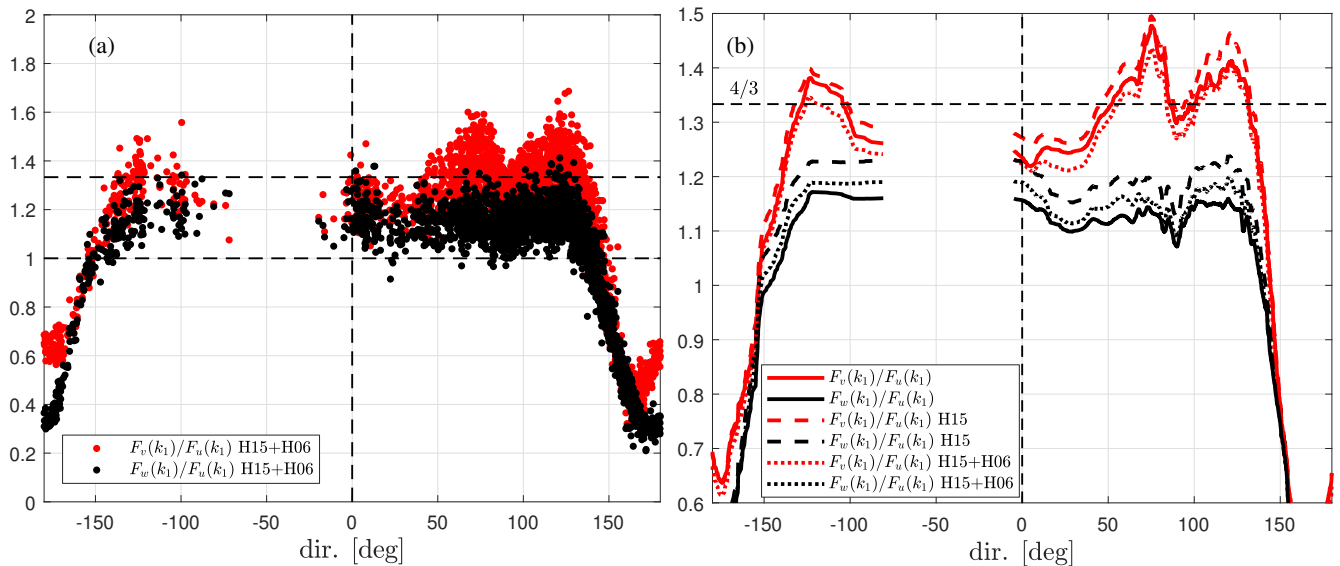


Figure 7. Velocity spectra ratios by the CSAT3 at the Risø test site as a function of wind direction for each 10-min period after applying the corrections in H15 and H06 (left frame a) and averaged over five degree intervals loess fits of the scatter (right frame b). Horizontal and vertical dashed lines as in Fig. 4. The standard error of the fit to the w - to u -velocity spectra ratios is within 0.0024–0.0072

5.3 CSAT3 at the Nørrekær Enge wind farm

Figure 8 shows two examples of normalized velocity spectra, ensemble-averaged over two direction intervals for measurements of the CSAT3 at Nørrekær Enge as well as the polynomial fit within a chosen wavenumber range. ~~Due to noise at the highest~~ The wavenumber range was limited to exclude noise apparent at higher wavenumbers ($k_1 > 1 \text{ m}^{-1}$), ~~we limit the range to a~~ close to noise-free wavenumber. Similar to the velocity spectra measured by the CSAT3 at the Risø test site, the w spectrum ~~follows followed~~ closely the u spectrum and the v spectrum ~~shows showed~~ the highest spectral density within the inertial subrange ($0.38 \text{ m}^{-1} \leq k_1 \leq 0.88 \text{ m}^{-1}$).

Figure 9 shows the w and v to u spectra ratios for each 10 min. The result is very similar to that for the CSAT3 at the Risø test site where within a range of directions of $\pm 150^\circ$, the w to u spectra ratios ~~are were~~ close to one, whereas the v to u spectra

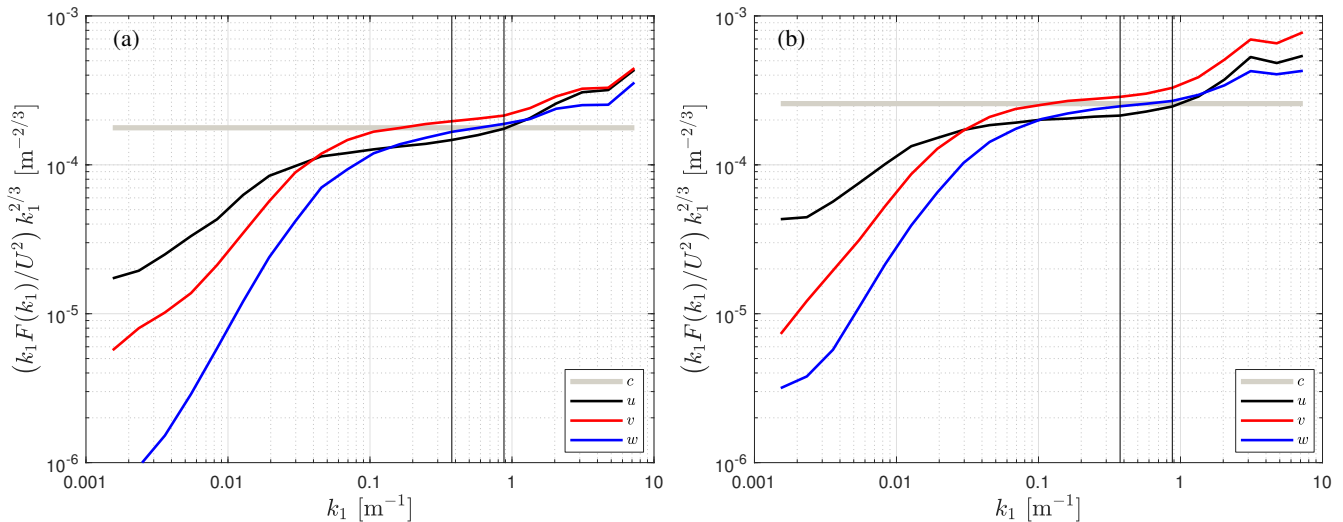


Figure 8. Similar to Fig. 3 but for the CSAT3 at the Nørrekær Enge wind farm

ratios are were close to 4/3. The boom/mast structure has had a greater effect on the CSAT3 at the Nørrekær Enge wind farm than at the Risø site as expected due to the setup. For both sites, the effect of the boom/mast at directions close to $\pm 180^\circ$ is was very similar. In agreement with the findings using the CSAT3 at Risø (Sect. 5.2), the H15 correction increases increased both the $F_w(k_1)/F_u(k_1)$ and $F_v(k_1)/F_u(k_1)$ spectra ratios (particularly for the former) but not enough to reach the 4/3 value for $F_w(k_1)/F_u(k_1)$ -(see Table 2). As for the previous two cases, for all correction types and criteria, the v - to u -spectra ratio was close to 4/3.

6 Discussion

6.1 Uncertainties

The aim of the spectral analysis displayed in Figs. 3, 6, and 8 was to find the optimal inertial subrange for each site and setup. A high-end limitation to this interval can be the presence of white noise in the spectra, which would tend to reduce the examined spectral ratios. For the velocity spectra at all three locations, we observe that the high frequency w -noise is the lowest of the three velocity components and is proportionally lower for the CSAT3 than for the USA-1, which is consistent with its larger path elevation angle as explained theoretically in Appendix B. According to the theory, the noise in the v - and u -spectra should be identical irrespective of the wind direction relative to the boom. The data showed deviations from this prediction. In addition, for the Risø CSAT3 setup, numerous tests with regards to both wavenumber and frequency ranges were tested performed, resulting in only very slight changes to the results in Fig. 7 (not shown). Another test for the robustness of the results was performed by selecting only those spectra ,-which that showed close to perfect inertial subrange behavior within

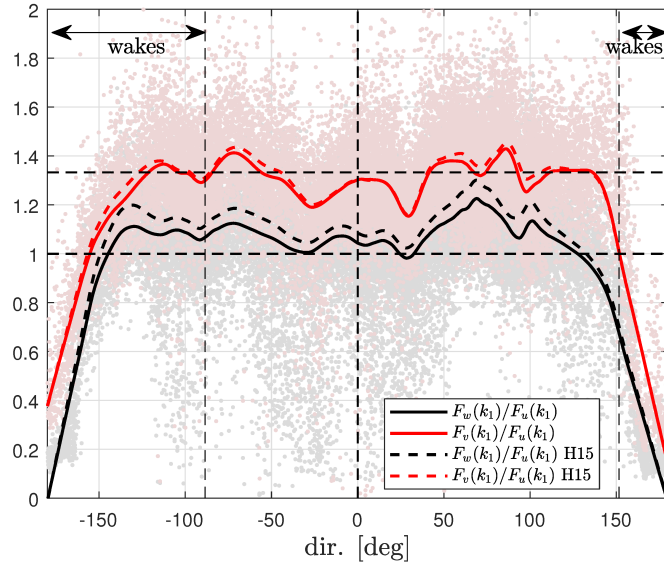


Figure 9. CSAT3 velocity spectra ratios with wind direction at the Nørrekær Enge wind farm. Horizontal and vertical dashed lines as in Fig. 4. The standard error of the fit to the w - to u -velocity spectra ratios is within 0.0038–0.0086 for the H15 correction

the selected wavenumber range (a close to $-5/3$ slope for $F_w(k_1)$) and a low **co-covariance** uw -co-covariance, see “sharpened criteria” in Table 2), which **affected the ratio** increased the CSAT3 ratios at Risø by 0.6–1.6% only.

The choice of thresholds for the sharpened criteria compromised the amount of data left for the analysis; about 4%, 25%, and 1% of the original amount of 10-min periods for the USA-1 at Risø, CSAT3 at Risø and the CSAT3 at Nørrekær Enge,
 5 respectively. The choice, however, did not change the velocity spectra ratios significantly. The softening of the values to, e.g., 0.03 and 0.2 for the w -spectral slope and the uw -co-covariance, respectively, resulted in a change of the w - to u -velocity spectra ratio of ≈ 0.5 – 1.5 %– 0.6 % for the USA-1, ≈ 1.5 % for the CSAT3 at Risø, and ≈ 0.8 % for the CSAT3 at Nørrekær Enge,
 only.

Another potential source of error comes from the choice of coordinate system in which the spectra **are-were** calculated.
 10 Here, we used two rotations for each 10-min block of data, whereas Horst et al. (2015) used the planar-fit coordinate system by Wilczak et al. (2001). We tested whether an error in rotation angle would change the results. This was done by rotating the sonic anemometer measurements of the velocity components and applying an isotropic inertial subrange 3D spectral velocity tensor, as in H06, to calculate the nominal component spectra for this configuration. A change of up to $\pm 5^\circ$ in the rotation angles of the sonic anemometer about vertical and transverse axes resulted in a less than 0.7% reduction in the spectral ratio;
 15 therefore, we consider rotation-related errors to be of no importance.

6.2 Implications

We base our analysis on theoretical arguments about the w - and v - to u -velocity spectral ratios, which should be equal to $4/3$ within the inertial subrange. We find such ratios by applying the 3D wind-tunnel-derived flow-distortion corrections to atmospheric velocity measurements performed with a USA-1 (Table 2); whereas applying a flow distortion correction to the CSAT3 results in ratios within the range 1.12–1.19. ~~Assuming that this discrepancy~~ If we assume that the discrepancy to $4/3$ is due to remaining uncorrected flow distortion and further ~~by assuming~~ , that flow distortion affects the observed frequencies equally, which ~~was supported by Huq et al. (2017)~~ is an assumption supported by the results presented in Huq et al. (2017), the imperfect ratios correspond directly to ~~underestimations in~~ underestimation in the velocity variances. ~~Hence, the results in Table 2 can be used~~ Since our results do not indicate how each velocity component is affected, it is still difficult to directly use the results presented here to correct the CSAT3's $F_w(k_1)/F_u(k_1)$ ratio to variances. However, some qualitative comparisons can be made. If, for example, the u - and v velocity components are measured with no error, the observed ratios of 1.12–1.19 can only turn into $4/3$. ~~If we assume that the error is only affecting the w component, we can estimate the correction by dividing the ideal ratio with the observed ratio (Table 2). Using the observed CSAT3 ratios for Risø and Nørrekær Enge without any correction applied,~~ 3 if the w variance ~~should then increase~~ is increased by 18–26%, which means that the w component itself should increase by 8–12%. ~~These error ranges are~~ This error range is in agreement with the results by Frank et al. (2016), and significantly higher than those suggested by Huq et al. (2017). A drawback with the method is, however, that it is not possible to determine which of the velocity components is affected. The ideal ratio can also be achieved, e.g., by assuming an 4–6% error ~~Frank et al. (2016), but higher than the error suggested by Huq et al. (2017). If we, on the other hand, assume equal errors on all velocity components (positive for u and v , and negative for w)~~ the ideal ratio of $4/3$ can be reached with a 4–6% correction on the velocity components. These examples illustrate that our method can be a useful tool for judging whether flow distortion corrections of a particular sonic anemometer are adequate or not, but that it cannot be used directly to quantify the error.

Another clear result from the presented analyses concerns the difference between observed mast/boom/instrument shadowing for the USA-1 and CSAT3; even from narrow masts and relatively long supporting booms, the mast influence is more marked for the CSAT3 than for the USA-1. Whereas Foken (2008) recommended the use of sonic anemometers without a pole directly under the sonic measurement volume for atmospheric turbulence research, we here stress that this statement can at best be valid only for a limited wind direction interval. For anemometers mounted on bulky walk-up towers, the direction interval where data will be biased from the tower will likely be much larger. We further stress that a sonic anemometer that cannot reproduce a $4/3$ ratio in the inertial subrange cannot be trusted to give accurate observations of all velocity components, provided that an inertial subrange is clearly apparent. Despite a higher ratio of transducer diameter to path length, which is sometimes used as a sonic anemometer quality marker, the USA-1, including the wind-tunnel-derived flow distortion correction, therefore comes out better from our analysis.

6.3 ~~References in sonic~~ Sonic anemometry quality assessments

We suggest that the spectral ratios of velocity components within the inertial subrange are a valuable addition to field tests and wind-tunnel calibrations. The advantage of the presented method is that any sonic anemometer can be tested provided that inertial subrange characteristics are expected from the particular measurements. Unlike sonic anemometer intercomparisons, where ideal flat and uniform sites are preferred (e.g. Mauder et al., 2007), the spectral ratio method did not seem to be sensitive to the spatial and flow heterogeneity at the sites used here.

As mentioned above, a limitation to our method is that the accuracy of individual velocity components cannot be assessed; the 3D-corrected observations from the USA-1, although almost perfect in terms of the 4/3 ratio, might still be inaccurate if all three velocity components are biased. Looking ahead, a ~~further~~ reference for sonic anemometer measurements could be found in small-volume lidar anemometry (Abari et al., 2015), which is free of flow distortion.

6.4 Can wind-tunnel based calibrations be trusted in atmospheric turbulence?

Starting with Högström and Smedman (2004), the validity of wind-tunnel calibrations for sonic anemometer has been questioned for applications in the turbulent atmosphere. Using large-eddy simulation results, Huq et al. (2017) argued that the magnitude of flow-distortion error caused by the sonic anemometer is smaller under turbulent conditions than under quasi-laminar flow, while also showing that the flow-distortion error does not depend on the frequency of the fluctuations. Taken the latter result to the extreme low-frequency limit, these two results appear inconsistent. In this study, the application of a flow-distortion correction for the USA-1, derived from wind-tunnel observations, led to near-perfect spectral ratios in the inertial subrange, whereas that by H15, based on both field tests and wind-tunnel observations, did not. Provided that the wind-tunnel reference instrument is accurate and the blockage ratio in the tunnel is small, we argue that flow distortion can be correctly quantified also in quasi-laminar flow, because the turbulence eddy sizes are significantly larger than the transducer size. In this way, the atmospheric turbulent flow appears laminar as seen from the transducer. An explanation for the deviation of the results between sonic anemometer observations in wind tunnel and field tests in Högström and Smedman (2004) could also be that the velocities recorded by the early Gill sonic anemometers showed a marked temperature dependence (Mortensen and Højstrup, 1995).

25 7 Conclusions

The accuracy of atmospheric turbulence measurements performed by sonic anemometers was investigated using two instruments, a CSAT3 and a USA-1, at two locations in Denmark. This was achieved by computing velocity spectra ratios within the inertial subrange. ~~We propose to perform such an analysis, in addition to field site intercomparisons and wind-tunnel calibrations, as a method to assess the accuracy of sonic anemometer measurements.~~ It was found that 3D flow corrections applied to measurements from the USA-1 helped recovering the 4/3 ratio of the w - to the u -velocity spectra that is expected within the inertial subrange. The 3D corrections also have a strong influence on the estimated w -variances, which are systemat-

ically found to be $\approx 4/3$ 33.33% higher than those of the uncorrected values measurements. For the CSAT3, which is commonly categorized as the sonic anemometer closest to be a distortion-free instrument, the ratio of the w - to the u -velocity spectra is ≈ 1.1 without applying a flow-distortion correction. Using a previously proposed flow-distortion correction, the ratios changed to ≈ 1.15 on average, pointing to that more work is needed to correctly quantify the flow distortion of this instrument. We propose to perform this type of analysis, in addition to field site intercomparisons and wind-tunnel calibrations, to assess the accuracy of sonic anemometer measurements. We also found that the influence of the mast, boom, and the instrument itself was higher on the CSAT3 compared to the USA-1 measurements.

Data availability. Sonic anemometer data are available under request to AP

Appendix A: Metek USA-1 3D flow-distortion corrections

Table A1. LUT for $\alpha_c(\alpha, \phi)$

ϕ [deg]	$C_{\alpha_c,0}$	$C_{\alpha_c,3}$	$S_{\alpha_c,3}$	$C_{\alpha_c,6}$	$S_{\alpha_c,6}$	$C_{\alpha_c,9}$	$S_{\alpha_c,9}$
-50	-10.7681	1.83694	8.12521	1.76476	-0.120656	-0.31818	1.30896
-45	-7.57048	2.25939	4.22328	-0.0394204	-0.112215	-0.289935	1.99387
-40	-6.77725	0.293479	3.05333	-1.16341	0.433886	0.207458	1.05195
-35	-4.12528	2.24741	0.286582	-0.936084	0.205636	-0.399336	1.57736
-30	-2.00728	3.63124	-0.325198	-0.821254	0.236536	-0.303478	0.854497
-25	-3.1161	3.91749	-0.682098	-0.274558	0.401386	-0.531782	0.470723
-20	-1.73949	3.5685	-0.253107	0.0306742	0.236975	-0.290767	-0.224723
-15	-2.59966	2.7604	-0.425346	0.0557135	0.0392047	0.222439	-0.364683
-10	-1.80055	2.02108	-0.259729	0.161799	0.117651	0.513197	-0.0546757
-5	-1.02146	1.22626	-0.469781	-0.177656	0.402977	0.408776	0.513465
0	0.152354	0.208574	0.051986	-0.102825	0.480597	-0.0710578	0.354821
5	0.310938	-0.703761	-0.0131663	0.0877815	0.546872	-0.342846	0.176681
10	0.530836	-1.68132	-0.0487515	0.0553666	0.524018	-0.426562	-0.0908979
15	1.70881	-2.46858	-0.487399	0.207364	0.638065	-0.458377	-0.230826
20	2.38137	-3.37747	0.026278	0.0749961	0.759096	0.105791	0.0287425
25	3.81688	-4.13918	-0.690113	0.170455	0.474636	0.424845	0.232194
30	3.49414	-3.82687	-0.229292	0.54375	0.322097	0.387805	0.823967
35	4.1365	-3.22485	0.752425	0.755442	0.623119	0.250988	1.26713
40	5.04661	-2.53708	1.23398	0.623328	0.653175	-0.359131	1.43131
45	4.26165	-3.12817	2.61556	0.0450348	-0.330568	-0.34354	0.81789

Table A2. LUT for $\phi_c(\alpha, \phi)$

ϕ [deg]	$C'_{\phi_e,0}$	$C'_{\phi_e,3}$	$S_{\phi_e,3}$	$C'_{\phi_e,6}$	$S_{\phi_e,6}$	$C'_{\phi_e,9}$	$S_{\phi_e,9}$
-50	5.77441	-2.19044	0.123475	-0.229181	0.226335	0.271943	0.0434668
-45	3.82023	-1.6847	0.315654	0.562738	0.175507	-0.0552129	-0.110839
-40	2.29783	-1.04802	0.0261005	0.239236	0.125053	-0.310631	0.388716
-35	1.37922	-1.0435	0.302416	-0.0112228	0.333846	-0.459678	0.172019
-30	0.837231	-0.593247	-0.199916	-0.0591118	0.19883	-0.307377	0.182622
-25	-0.0588021	-0.0720115	-0.6826	-0.253726	0.348259	-0.322761	0.0059973
-20	-0.0333721	0.101664	-1.41617	-0.136743	0.332169	-0.244186	-0.0612597
-15	0.0423739	0.0428399	-1.90137	-0.187419	0.148025	0.06782	-0.0317571
-10	0.318212	0.126425	-2.07763	-0.0341571	0.198621	0.178598	0.103543
-5	0.721731	-0.0274247	-2.10221	-0.081822	0.36773	0.0848013	0.184226
0	1.65254	-0.0582368	-2.18993	-0.0802346	0.234886	-0.0545883	-0.0092531
5	2.49129	-0.116475	-2.11283	0.112364	0.247405	-0.115218	-0.0682998
10	2.99839	-0.0867988	-2.04382	0.219581	0.207231	-0.0981521	-0.0581594
15	3.55129	-0.160112	-1.8474	0.22217	0.2794	-0.0323565	-0.0951596
20	3.20977	-0.137282	-0.966014	0.183032	0.380154	0.155093	-0.0557369
25	3.38556	-0.0596863	-0.898053	0.20526	0.39357	0.421141	-0.00842409
30	3.18846	0.266264	-0.0951907	0.166895	0.373018	0.338146	0.187917
35	2.60134	0.442007	0.211612	-0.114323	0.359926	0.224424	0.209482
40	2.04655	1.08915	0.470385	-0.333096	0.268349	0.263547	0.264963
45	0.987659	1.54127	0.815214	-0.504021	-0.0835985	0.197387	0.0819912

Table A3. LUT for $n_c(\alpha, \phi)$

ϕ [deg]	$C_{n_c,0}$	$C_{n_c,3}$	$S_{n_c,3}$	$C_{n_c,6}$	$S_{n_c,6}$	$C_{n_c,9}$	$S_{n_c,9}$
-50	1.23095	-0.0859199	-0.0674271	0.0160088	0.0363397	0.0141701	-0.0271955
-45	1.19323	-0.0430575	0.00309311	0.0430652	0.0225135	0.000740028	-0.0114045
-40	1.17255	-0.0206394	0.0145473	0.0399041	-0.00592748	-0.00650942	-0.00762305
-35	1.15408	-0.00768472	0.0614486	0.0382888	0.0123096	-0.0124673	-0.00598534
-30	1.12616	0.00000536	0.0636543	0.0386879	0.0153428	-0.014148	-0.000210096
-25	1.09976	0.00667086	0.0705414	0.0198549	0.0165582	-0.0114517	-0.00115495
-20	1.07518	0.00583915	0.0591098	0.011127	0.0104259	-0.00665653	0.00119842
-15	1.05173	0.00731099	0.0527018	0.00230123	0.00587927	-0.00229463	-0.00297294
-10	1.02428	0.00885121	0.0330304	-0.000597029	0.00340367	-0.000745781	-0.000283634
-5	1.011	0.00930375	0.0218448	-0.0046575	0.00203972	-0.00112652	0.00179908
0	1.00672	0.0105659	0.0034918	-0.00844128	0.00228384	-0.000824805	0.000200667
5	1.01053	0.00885115	-0.0182222	-0.00894106	-0.000719837	-0.000420398	-0.00049521
10	1.02332	0.00618183	-0.035471	-0.00455248	-0.00215202	-0.00229836	-0.000309162
15	1.04358	0.00648413	-0.0494223	0.000323015	-0.00396036	-0.00465476	-0.000117245
20	1.06928	0.00733521	-0.0638425	0.0101036	-0.00829634	-0.0073708	-0.00051887
25	1.09029	0.00396333	-0.0647836	0.0187147	-0.0126355	-0.0115659	0.000482614
30	1.11877	0.00299473	-0.0661552	0.0293485	-0.00957493	-0.00963845	0.0029231
35	1.13779	0.00812517	-0.0526322	0.0341525	-0.00971735	-0.0114763	0.0013481
40	1.16659	-0.00869651	-0.0537855	0.0290825	-9.89E+00	-0.0133731	0.0117738
45	1.18695	-0.0289647	-0.0461693	0.030231	-0.0121524	-0.00667729	0.00565286

Appendix B: Sonic anemometer noise

The transformation matrix to convert the three sonic path velocities $\mathbf{s} = (s_1, s_2, s_3)$, which are assumed positive from the lower to the upper acoustical transducer, to right-handed orthogonal velocity components $\mathbf{u} = (u_1, u_2, u_3) = (u, v, w)$ with u in the direction of the horizontal boom, v horizontal and transverse to u , and w vertical and positive upwards, is

$$5 \quad T = \begin{pmatrix} -\frac{2 \sec \phi_p}{3} & \frac{\sec \phi_p}{3} & \frac{\sec \phi_p}{3} \\ 0 & \frac{\sec \phi_p}{\sqrt{3}} & -\frac{\sec \phi_p}{\sqrt{3}} \\ \frac{\csc \phi_p}{3} & \frac{\csc \phi_p}{3} & \frac{\csc \phi_p}{3} \end{pmatrix}, \quad (\text{B1})$$

where ϕ_p is the path elevation angle, so

$$u_i = T_{ij} s_j, \quad (\text{B2})$$

and we also assume the sonic anemometer paths to be oriented in the azimuthal direction like the CSAT3 or the USA-1.

Suppose now that the sonic anemometer signals are composed of uncorrelated, white noise $\langle s_i s_j \rangle = \sigma_s^2 \delta_{ij}$, where δ is the
 10 Kronecker delta symbol and σ_s^2 is the noise variance. The resulting noise on the orthogonal velocity components then becomes

$$\begin{aligned} \langle u_i u_j \rangle &= \langle T_{ik} s_k T_{jl} s_l \rangle = \sigma_s^2 T_{ik} \delta_{kl} T_{jl} = \sigma_s^2 T_{ik} T_{jk} \\ &= \sigma_s^2 \begin{pmatrix} \frac{2 \sec^2 \phi_p}{3} & 0 & 0 \\ 0 & \frac{2 \sec^2 \phi_p}{3} & 0 \\ 0 & 0 & \frac{\csc^2 \phi_p}{3} \end{pmatrix} \end{aligned} \quad (\text{B3})$$

Since the u - and v -components behave identically in terms of noise, the error is also given by Eqn. (B3) if the components are rotated into the mean wind direction coordinate system and as long as the wind vector is horizontal. Also, since the
 15 noise is assumed white, the relative strengths of noise-dominated spectra will also follow Eqn (B3). The ratio between the horizontal and vertical spectra will therefore increase rapidly with path elevation angle as shown in Fig. B1. Unit ratio occurs for $\phi_p = \tan^{-1}(2^{-1/2}) \approx 35^\circ$ or at a path zenith angle of $90^\circ - \phi_p \approx 55^\circ$. This is also the path elevation angle where the sum of the three component variances obtains a minimum of exactly three times σ_s^2 . Because of flow distortion, sonic anemometers do not have such a low path elevation angle.

20 *Author contributions.* AP analyzed the USA-1 measurements at the Risø test site and the CSAT3 measurements at the Nørrekær wind farm. ED analyzed the CSAT3 measurements at the Risø test site. AP and ED contributed equally to the preparation of the paper. JM helped in the analysis and interpretation of the data and revised the contents of the manuscript. ED and JM came up with the idea of using the velocity spectra to diagnose flow-distortion effects on the sonic anemometer measurements

Competing interests. The authors declare that they have no conflict of interest

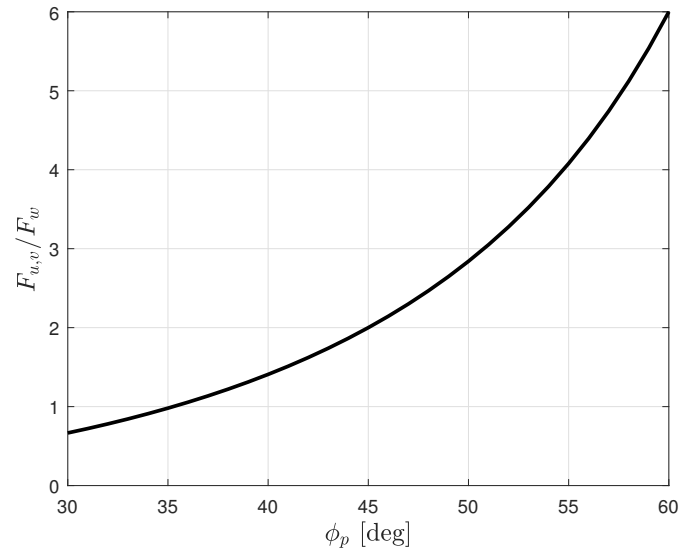


Figure B1. The ratio of the noise level in the horizontal velocity components to the vertical one as a function of path elevation angle

Acknowledgements. We would like to thank the technical support of the Test and Measurements section at DTU Wind Energy and in particular to Søren W. Lund. ED would like to thank the TrueWind project, which is funded by the Energy Technology Development and Demonstration Program (EUDP), Denmark for financial support. Finally, we would like to thank Tom Horst for many inspiring discussions on flow distortion corrections.

References

- Abari, C., Pedersen, A., Dellwik, E., and Mann, J.: Performance evaluation of an all-fiber image-reject homodyne coherent Doppler wind lidar, *Atmospheric Measurement Techniques*, 8, 2015.
- Dimitrov, N., Natarajan, A., and Kelly, M.: Model of wind shear conditional on turbulence and its impact on wind turbine loads, *Wind Energ.*, 5 18, 1917–1931, 2015.
- Dyer, A. J.: Flow distortion by supporting structures, *Boundary-Layer Meteorol.*, 20, 243–251, 1981.
- Foken, T.: the Energy Balance Closure Problem: an Overview, *Ecological Applications*, 18, 1351–1367, 2008.
- Frank, J. M., Massman, W. J., and Ewers, B. E.: Underestimates of sensible heat flux due to vertical velocity measurement errors in non-orthogonal sonic anemometers, *Agr. Forest Meteorol.*, 171–172, 72–81, 2013.
- 10 Frank, J. M., Massman, W. J., and Ewers, B. E.: A Bayesian model to correct underestimated 3-D wind speeds from sonic anemometers increases turbulent components of the surface energy balance, *Atmos. Meas. Tech.*, 9, 5933–5953, 2016.
- Grelle, A. and Lindroth, A.: Flow distortion by a Solent sonic anemometer: wind tunnel calibration and its assessment for flux measurements over forest and field, *J. Atmos. Ocean. Technol.*, 11, 1529–1542, 1994.
- Högström, U. and Smedman, A.-S.: Accuracy of sonic anemometers: laminar wind-tunnel calibrations compared to atmospheric *in situ* 15 calibrations against a reference instrument, *Boundary-Layer Meteorol.*, 111, 33–54, 2004.
- Horst, T. W. and Oncley, S. P.: Corrections to inertial-range power spectra measured by CSAT3 and Solent sonic anemometers, 1. Path-averaging errors, *Boundary-Layer Meteorol.*, 119, 375–395, 2006.
- Horst, T. W., Semmer, S. R., and Maclean, G.: Correction of a non-orthogonal, three-component sonic anemometer for flow distortion by transducer shadowing, *Boundary-Layer Meteorol.*, 155, 371–395, 2015.
- 20 Huq, S., De Roo, F., Foken, T., and Mauder, M.: Evaluation of probe-induced flow distortion of Campbell CSAT3 sonic anemometers by numerical simulation, *Boundary-Layer Meteorol.*, 165, 9–28, 2017.
- Ibrom, A., Dellwik, E., Larsen, S., and Pilegaard, K.: On the use of the Webb-Pearman-Leuning theory for closed-path eddy correlation measurements, *Tellus, Series B: Chem. Phys. Meteorol.*, 59, 937–946, 2007.
- Kaimal, J. C. and Finnigan, J. J.: *Atmospheric boundary layer flows: Their structure and measurement*, Oxford University press, 1994.
- 25 Kaimal, J. C., Wyngaard, J. C., and Haugen, D. A.: Deriving power spectra from a three-component sonic anemometer, *J. Appl. Meteor.*, 7, 827–837, 1968.
- Kaimal, J. C., Gaynor, J. E., Zimmerman, H. A., and Zimmerman, G. A.: Minimizing flow distortion errors in a sonic anemometer, *Boundary-Layer Meteorol.*, 53, 103–115, 1990.
- Kochendorfer, J., Meyers, T. P., Frank, J., Massman, W. J., and Heuer, M. W.: How well can we measure the vertical wind speed? Implication 30 for fluxes of energy and mass, *Boundary-Layer Meteorol.*, 145, 383–398, 2012.
- Kolmogorov, A. N.: The local structure of turbulence in incompressible viscous fluid for very large Reynolds number, *Doklady ANSSSR*, 30, 301–304, 1941.
- Kraan, C. and Oost, W. A.: A new way of anemometer calibration and its application to a sonic anemometer, *J. Atmos. Ocean. Technol.*, 6, 516–524, 1989.
- 35 Mauder, M., Oncley, S. P., Vogt, R., Weidinger, T., Ribeiro, L., Bernhofer, C., Foken, T., Kohsiek, W., Bruin, H. A. R. D., and Liu, H.: The energy balance experiment EBEX-2000. Part II: intercomparison of eddy-covariance sensors and post-field data processing methods, *Boundary-Layer Meteorol.*, 123, 29–54, 2007.

- McCaffrey, K., Quelet, P. T., Choukulkar, A., Wilczak, J. M., Wolfe, D. E., Oncley, S. P., Brewer, W. A., Debnath, M., Ashton, R., Iungo, G. V., and Lundquist, J. K.: Identification of tower-wake distortions using sonic anemometer and lidar measurements, *Atmos. Meas. Tech.*, 10, 393–407, 2017.
- Metek GmbH: Flow distortion correction for 3-d flows as measured by METEK's ultrasonic anemometer USA-1, 2004.
- 5 Meyers, T. P. and Heuer, M.: A field methodology to evaluate sonic anemometer angle of attack errors, in: 27th Conference on Agric. For. Meteorol., San Diego, California, 2006.
- Mortensen, N. and Højstrup, J.: The Solent sonic - response and associated errors, Ninth Symposium on Meteorological Observations and Instrumentation, pp. 501–506, 1995.
- Mortensen, N. G.: Flow-Response Characteristics of the Kaijo Denki Omni-Directional · Sonic Anemometer (TR-61B), Tech. rep., Forskningscenter Risoe, Denmark, 1994.
- 10 Mücke, T., Kleinhans, D., and Peinke, J.: Atmospheric turbulence and its influence on the alternating loads on wind turbines, *Wind Energ.*, 14, 301–316, 2011.
- Nakai, T. and Shimoyama, K.: Ultrasonic anemometer angle of attack errors under turbulent conditions, *Agric. For. Meteorol.*, 162-163, 14–26, 2012.
- 15 Pope, S. B.: *Turbulent Flows*, Cambridge University Press, New York, 2000.
- van der Molen, M. K., Gash, J. H. C., and Elbers, J. A.: Sonic anemometer (co)sine response and flux measurement: II. The effect of introducing an angle of attack dependent calibration, *Agr. Forest Meteorol.*, 122, 95–109, 2004.
- Wilczak, J. M., Oncley, S. P., and Stage, S. A.: Sonic anemometer tilt correction algorithms, *Boundary-Layer Meteorol.*, 99, 127–150, 2001.
- Wyngaard, J. C.: The effects of probe-induced flow distortion on atmospheric measurements, *J. Appl. Meteorol.*, 20, 784–794, 1981.
- 20 Wyngaard, J. C. and Zhang, S.-F. F.: Transducer-Shadow Effects on Turbulence Spectra Measured by Sonic Anemometers, *J. Atmos. Ocean. Technol.*, 2, 548–558, 1985.
- Zhang, S. F., Wyngaard, J. C., Businger, J. A., and Oncley, S. P.: Response characteristics of the U.W. sonic anemometer, *J. Atmos. Ocean. Technol.*, 3, 315–323, 1986.